15. NINETYEAST RIDGE SUMMARY[1]

Shipboard Scientific Party[2]

INTRODUCTION

Deep Sea Drilling Project (DSDP) drilling on the Ninetyeast Ridge in 1972 provided confirmation that the origin of the ridge was related to hot-spot volcanism from the Kerguelen-Heard Plume. However, many important geochemical and tectonic questions remained open because of the limited data available.

The Ocean Drilling Program (ODP) Leg 121 drilling program on Ninetyeast Ridge was designed to add three more sites on this 5000-km-long feature, with a particular emphasis on much deeper penetration of basement than had been achieved previously. Even with the eight sites now on the ridge, the average spacing between sites is still 650 km, and basement rocks have not been sampled at all on the northern 1200-km section of the ridge (Fig. 1).

The general objectives of the Ninetyeast Ridge drilling program can be summarized as follows:

1. To study the geochemical relationships in time and space between Ninetyeast Ridge and the Kerguelen-Heard Plume.
2. To derive a detailed paleomagnetic northward-motion curve for the Indian plate with particular emphasis on the Paleogene as the period of initial collision between the Indian and Asian plates.
3. To provide a south-north paleontological and paleoclimatological transect of the eastern Indian Ocean at a depth shallower than the carbonate compensation depth.

This chapter summarizes the early scientific results of the shipboard studies. Many other objectives await the post-cruise analysis of samples from Leg 121 and synthesis of the results from all of the ODP legs in the Indian Ocean.

Our understanding of the tectonic and geochemical history of the Kerguelen-Heard Plume is much improved as a result of ODP drilling on its three traces, Ninetyeast Ridge (ODP Leg 121), Broken Ridge (ODP Leg 121), and the Kerguelen-Heard Plateau (ODP Legs 119 and 120). In particular, the shipboard scientific results from the Ninetyeast Ridge drilling have provided new perspectives into the variability of eruptive mechanisms and geochemical trends along the ridge. These results are summarized in this chapter in four sections: "Lithostratigraphy and Sedimentology," "Tephra," "Igneous Petrology," and "Geochemistry." The tectonic implications of these results are outlined in the "Conclusions" section.

LITHOSTRATIGRAPHY AND SEDIMENTOLOGY

Biogenic Sediments, Sedimentation Rates, and Fluxes

The sedimentary sequences of the three sites drilled along Ninetyeast Ridge during Leg 121—Site 756 at about 27°S, Site 757 at about 17°S, and Site 758 at about 5.5°N—are all similar in lithology. Nannofossil ooze with varying amounts of foraminifers grades down into chalks at Sites 757 and 758 and overlies basalt at Site 756 and ash/tuff sequences at Sites 757 and 758. The ooze is essentially pure carbonate at the two southern sites, but is diluted with terrigenous clay in upper Miocene to Pleistocene sediments at the northernmost site. The upper Miocene sediments of Site 758 also contain rare to common radiolarians.

The nannofossil zonations allow calculation of linear sedimentation rates for the Maestrichtian through Pleistocene sediments. The mass-accumulation rate of these same materials, measured in $g/cm^2/1000$ yr, was determined by multiplying the linear sedimentation rate in cm/1000 yr by the dry-bulk density in g/cm^3. The flux patterns thus determined show a general similarity among the three sites (Table 1 and Fig. 2). All sites show relatively higher fluxes of pelagic sediment in the late Miocene to Pleistocene part of the record, beginning at about 9 Ma.

The middle and early Cenozoic record varies somewhat. At Site 758 most of the Eocene is condensed or missing, a condition that prevailed between 35 and 55 Ma (represented as a very low accumulation rate in Table 1). Eocene sediments accumulated at approximately 0.5 to 0.6 $g/cm^2/1000$ yr at Site 757, but much of the Oligocene is greatly condensed or missing at that site. Site 756 had fairly low fluxes throughout the middle Cenozoic, of about 0.3 $g/cm^2/1000$ yr, but the sediment column appears to be continuous down through the Oligocene.

The Eocene through middle Miocene periods of low to no sediment flux that occur at all of the Ninetyeast Ridge drill sites cover a broad range of space and time (Fig. 3). These low fluxes occurred at paleopositions beneath the Southern Hemisphere subtropical gyre, roughly 10°S to 40°S, between 9 and 58 m.y. ago. The late Miocene flux increase, in contrast, is a sharp demarcation that occurs at the same time everywhere on Ninetyeast Ridge. The biostratigraphy is consistent with a sudden, roughly four-fold increase in the flux of ooze at 9 Ma. This time of the earlier part of the late Miocene was one of increased sedimentation rate in the equatorial Pacific as well as the Indian Ocean and presumably reflects an increase in the vigor of ocean circulation with concomitant enhanced upwelling and productivity.

At the northern Site 758, terrigenous materials make up an important percentage of the sediments. There, in materials younger than the Eocene hiatus, the noncarbonate component averages approximately 15% in Oligocene through early Miocene age sediment and 20% in middle Miocene sediment. The mass-accumulation rate of the terrigenous component for these times is 0.05 to 0.08 $g/cm^2/1000$ yr. It was not until about 8 Ma that the flux of mud increased above these background levels, to a value of 0.4 $g/cm^2/1000$ yr for the past 4 m.y.

Three things happened at about 8 Ma that may account for this flux increase. First, Site 758, which has always been on the same plate as India, drifted northward across the equator, and thus increased its accessibility to northern-source terrigenous material. Second, biogenic sediment flux regionally increased, as previously described, at that time. Third, in addition to the increase in overall fluxes, the relative amount of terrigenous material also increased. When the percentage of a dilutant in-

[1] Peirce, J., Weissel, J., et al., 1989. *Proc. ODP, Init. Repts.*, 121: College Station, TX (Ocean Drilling Program).

[2] Shipboard Scientific Party is as given in the list of Participants preceding the contents, with the addition of Jean-Yves Royer, Institute for Geophysics, University of Texas at Austin, 8701 Mopac Boulevard, Austin, TX 78759-8345.

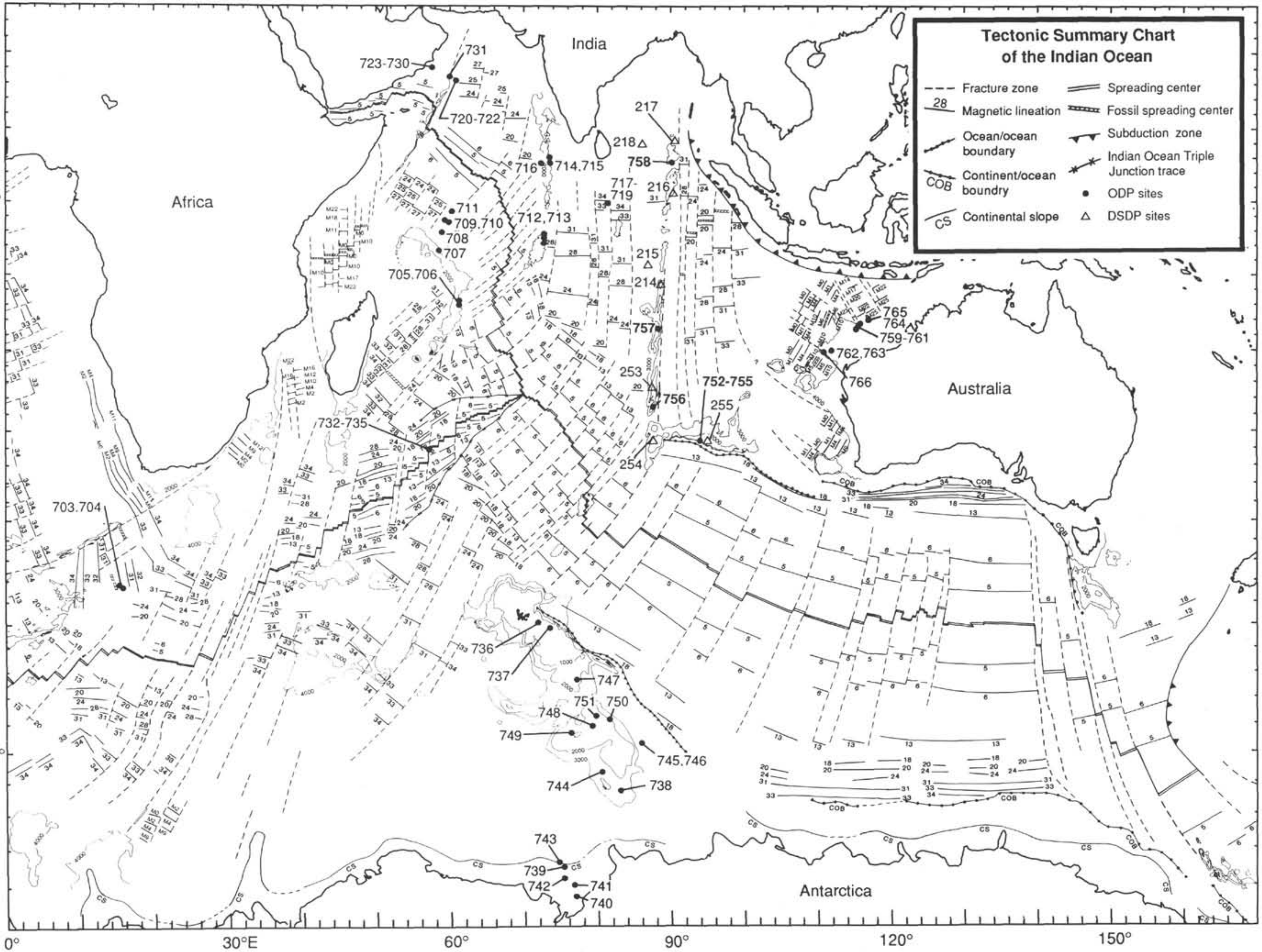

Figure 1. Index map of the Indian Ocean, showing major bathymetric plateaus and ridges, magnetic anomalies, and DSDP/ODP sites (after Royer et al., in press).

Table 1. Sedimentation rates and fluxes for Ninetyeast Ridge Sites 756, 757, and 758.

Age (Ma)	ΔT (m.y.)	Depth (mbsf)	ΔZ (m)	Linear sedimentation rate (cm/1000 yr)	Dry-bulk density (g/cm^3)	Mass-accumulation rate (g/cm^2/1000 yr)
Site 756						
0–1.90	1.90	0–1.19	1.19	0.06	1.10	0.07
1.90–3.50	1.60	1.19–5.25	4.06	0.25	1.08	0.27
3.50–3.80	0.30	5.25–8.25	3.0	1.00	1.08	1.08
3.80–8.85	5.05	8.25–35.19	26.94	0.53	1.12	0.60
8.85–10.0	1.15	35.19–38.05	2.86	0.25	1.10	0.27
10.0–14.4	4.4	38.05–46.15	8.10	0.18	1.11	0.20
14.4–17.1	2.7	46.15–55.45	9.30	0.34	0.98	0.34
17.1–25.2	8.1	55.45–74.20	18.75	0.23	1.12	0.26
25.2–34.6	9.4	74.20–118.45	44.25	0.47	1.23	0.58
34.6–36.7	2.1	118.45–135.65	17.20	0.82	1.18	0.97
Site 757						
0–0.474	0.474	0–3.05	3.05	0.64	0.78	0.50
0.474–1.45	0.976	3.05–9.75	6.70	0.69	0.78	0.54
1.45–1.90	0.45	9.75–12.75	3.00	0.67	0.92	0.62
1.90–2.60	0.70	12.75–16.25	3.50	0.50	0.89	0.45
2.60–3.80	1.20	16.25–27.35	11.10	0.93	0.94	0.87
3.80–5.00	1.20	27.35–38.95	11.60	0.97	1.03	1.00
5.00–5.60	0.60	38.95–43.55	4.60	0.77	1.02	0.79
5.60–6.50	0.90	43.55–53.25	9.70	1.08	1.12	1.21
6.50–8.20	1.70	53.25–62.90	9.65	0.57	1.21	0.69
8.20–8.85	0.65	62.90–71.50	8.60	1.32	1.10	1.45
8.85–13.10	4.25	71.50–81.20	9.70	0.23	1.19	0.27
13.10–14.40	1.30	81.20–83.75	2.55	0.20	1.24	0.25
14.10–15.40	1.00	83.75–89.75	6.00	0.60	1.10	0.66
15.40–17.10	1.70	89.75–96.45	6.70	0.39	1.28	0.50
17.10–21.50	4.40	96.45–99.45	3.00	0.07	1.24	0.09
21.50–23.20	1.70	99.45–100.50	1.05	0.06	1.19	0.07
23.20–23.70	0.50	100.50–101.55	1.05	0.21	1.25	0.26
23.70–30.20	6.50	101.55–106.05	4.50	0.07	1.25	0.09
30.20–34.2	4.00	106.05–111.25	5.20	0.13	1.20	0.16
34.2–35.1	0.90	111.25–119.80	8.55	0.95	1.34	1.27
35.1–36.7	1.60	119.80–123.85	4.05	0.25	1.40	0.35
36.7–37.8	1.10	123.85–129.45	5.60	0.51	1.37	0.70
37.8–40.0	2.20	129.45–132.55	3.10	0.14	1.38	0.19
40.0–45.4	5.40	132.55–154.35	21.80	0.40	1.46	0.58
45.4–47.0	1.60	154.35–159.15	4.80	0.30	1.44	0.43
47.0–48.8	1.80	159.15–166.75	7.60	0.42	1.62	0.68
48.8–49.8	1.00	166.75–175.00	8.25	0.82	1.63	1.34
49.8–52.6	2.80	175.00–186.45	11.45	0.41	1.68	0.69
52.6–53.7	1.10	186.45–202.75	16.30	1.48	1.64	2.43
53.7–55.3	1.60	202.75–212.45	9.70	0.61	1.37	0.84
Site 758						
0–0.474	0.474	0.0–6.75	6.75	1.42	0.73	1.04
0.474–1.37	0.896	6.75–16.35	9.6	1.07	0.78	0.83
1.37–1.90	0.53	16.35–25.95	9.6	1.81	0.82	1.48
1.90–2.20	0.30	35.95–34.05	8.1	2.70	0.91	2.46
2.20–2.90	0.70	34.05–38.55	4.5	0.64	0.88	0.56
2.90–3.80	0.90	38.55–57.75	19.2	2.13	0.90	1.92
3.80–5.60	1.80	57.75–70.45	12.7	0.71	0.95	0.67
5.60–6.50	0.90	70.45–83.85	13.4	1.49	0.97	1.45
6.50–8.85	2.35	83.85–117.35	33.5	1.43	1.04	1.49
8.85–17.40	8.55	117.35–144.75	27.4	0.32	1.02	0.33
17.40–25.20	7.80	144.75–196.05	51.3	0.66	1.00	0.66
25.20–30.20	5.00	196.05–219.05	23.0	0.46	1.07	0.49
30.20–34.20	4.00	219.05–238.45	19.4	0.48	1.08	0.52
[a]34.20–59.20	25.00	238.45–264.75	26.3	0.11	1.29	0.14
59.20–60.4	1.20	264.75–271.35	6.6	0.55	1.31	0.72
60.4–62.0	1.60	271.35–291.00	19.65	1.23	1.37	1.69
62.0–64.8	2.80	219.00–293.85	2.85	0.10	1.32	0.13
64.8–69.0	4.20	293.85–295.85	2.00	0.05	1.26	0.06

[a] Hiatus.

creases at the same time the flux of the dominant sedimentary component increases, then the dilutant material is representative of an important sediment source.

The Leg 121 Scientific Party will attempt to define a relationship between the terrigenous component in the Cenozoic sediments of Site 758 and erosion and runoff from the Himalayas. Erosion would be enhanced by an increase in relief of the mountains or by an increasing severity of climate. A simple interpretation of the flux data, then, is that prior to 35 Ma and again at about 9 Ma some change in uplift and/or climate occurred, each of which served to increase the flux of terrigenous material to the location of Site 758. This latter event, unfortu-

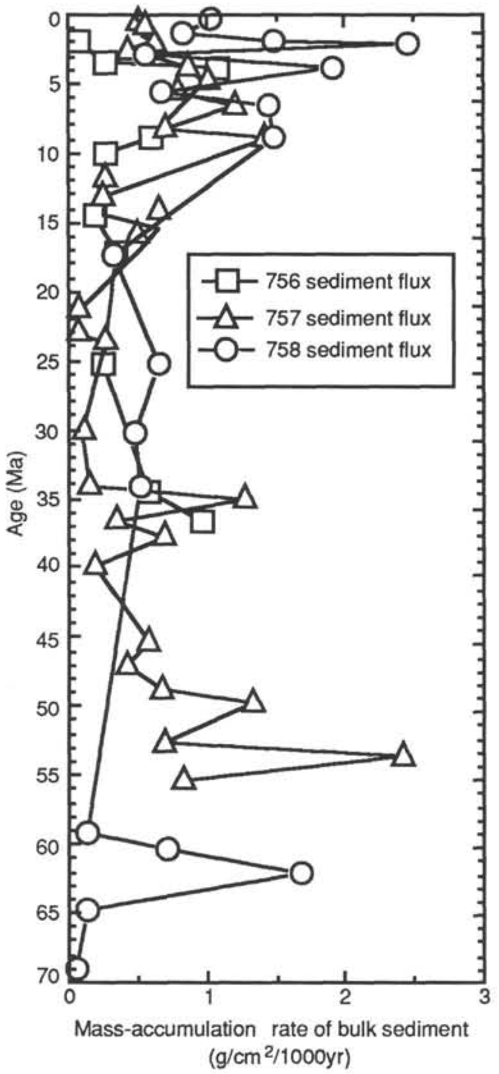

Figure 2. Sediment flux at Sites 756, 757, and 758.

nately, becomes equivocal because it coincides in time with the passage of the site below the equator (Fig. 3). Because of the greater vertical flux of organic debris and aggregates associated with the high-productivity zone, the equator acts as a barrier to cross-equatorial transport of particles as they are swept from the water by the increased organic rain. The relative importance of this process could not be determined aboard ship; it remains for laboratory studies to determine the relative abundance of northern-source, presumably Himalayan, terrigenous materials in sediments deposited south of the equator. Thus, the time of 9 Ma for the beginning of increased fluxes of the terrigenous component constrains only the young end of the range of age estimates for this late Miocene uplift/climatic event.

TEPHRA

Volcanic glass is a common component of the sediments recovered at Sites 757 and 758 during drilling on Ninetyeast Ridge. Glass is present only in trace amounts at Site 756, and no individual ash layers were observed. Many discrete layers are present at Sites 757 and 758. The ash layers provide important stratigraphic markers for correlation among the holes at each site, as well as providing information on eruptive style and history of Ninetyeast Ridge. The Miocene to Holocene ashes recovered at Site 758 record the tephrochronology of the Indonesian volcanic arc.

Lithology

Traces of volcanic glass are common in most cores from Sites 757 and 758. At Site 757, the glass content, as well as the amount of clay, increases in the early Eocene age and older rocks to more than 10% in Core 121-757B-23X. At Site 758 the ash common in the first few piston cores (121-758A-1H, 121-758B-1H, and 121-758C-1H) is assumed to be derived from the Indonesian arc. Glass content decreases downhole to trace amounts, with only isolated ash layers in the upper Campanian. Within the Campanian section ash content increases to consistently more than 10% in Core 121-758A-41X. The absence of ash layers at Site 756 may be the result of erosion or slumping of these layers from the underlying basalt before subsequent deposition of calcareous sediments (see "Lithostratigraphy and Sedimentology" section, "Site 756" chapter, this volume). Conversely, there may not have been ash-generating eruptions after the youngest lava flow.

The volcanic materials recovered at Sites 757 and 758 are indicative of very different types of volcanism and can be categorized into three types:

1. Air-fall layers, which settled through the water column, occur both as discrete layers and as diffuse, bioturbated layers. The thickness of these layers is a function of the distance from the vent and the volume of erupted material.
2. Thick ash layers, composed of one or several composite ash falls, occur as very fine- to coarse-grained deposits that show layering, cross-bedding, and reworking. The thick layers also occur with hydroclastic accretionary lapilli aggregated into weak layers.
3. Thin (less than 2-m-thick) turbidity flow deposits of ash occur between lava flows.

The majority of the ashes recovered are basaltic or andesitic. Holocene ashes at Site 758 are silicic. Samples of the older ashes were taken for shipboard X-ray-fluorescence (XRF) analysis, and the results are tabulated and discussed in the "Igneous Petrology" sections of the "Site 757" and "Site 758" chapters (this volume).

Air-Fall Deposits

Air-fall deposits were seen in the most recent ash layers of Site 758. In Cores 121-758A-1H, 121-758A-2H, 121-758B-1H, 121-758B-2H, and 121-758C-1H these deposits occur as discrete ash layers within nannofossil oozes. The layers have sharp lower contacts and weakly gradational upper contacts. They are dark gray (10YR 4/1) to grayish brown (10YR 5/3) with black flecks of glass and crystals concentrated at the base of each layer. Some alteration is visible at depths greater than 3 m below the seafloor. The alteration usually occurs as green smectite clays, marking distinctive horizons in the cores. The refractive index of the clear glass fragments present in these layers indicates a silica content in excess of 60%. The glass shards are blocky and cuspate, appearing as bubble fragments or bubble walls. Generally, the shards have few vesicles, because of the great degree of fragmentation. The layers are well sorted and contain shattered and conchoidally fractured plagioclase crystals, indicating an extremely explosive environment such as a caldera collapse (Kennett, 1981). Optical properties of the plagioclase indicate a composition of An_{40} or less. The uppermost of the ash layers has been tentatively correlated with a major eruption approximately 75,000 yr ago from the Toba caldera (Ninkovich, 1979).

Basaltic air falls from vulcanian (maar-forming) or distal surtseyan (phreatic) eruptions are common deeper in the section. At Site 757 these first appear in the upper Eocene in Section 121-757B-23X-5 as layers less than 30 cm thick with sharp lower contacts and gradational, diffuse upper contacts. This

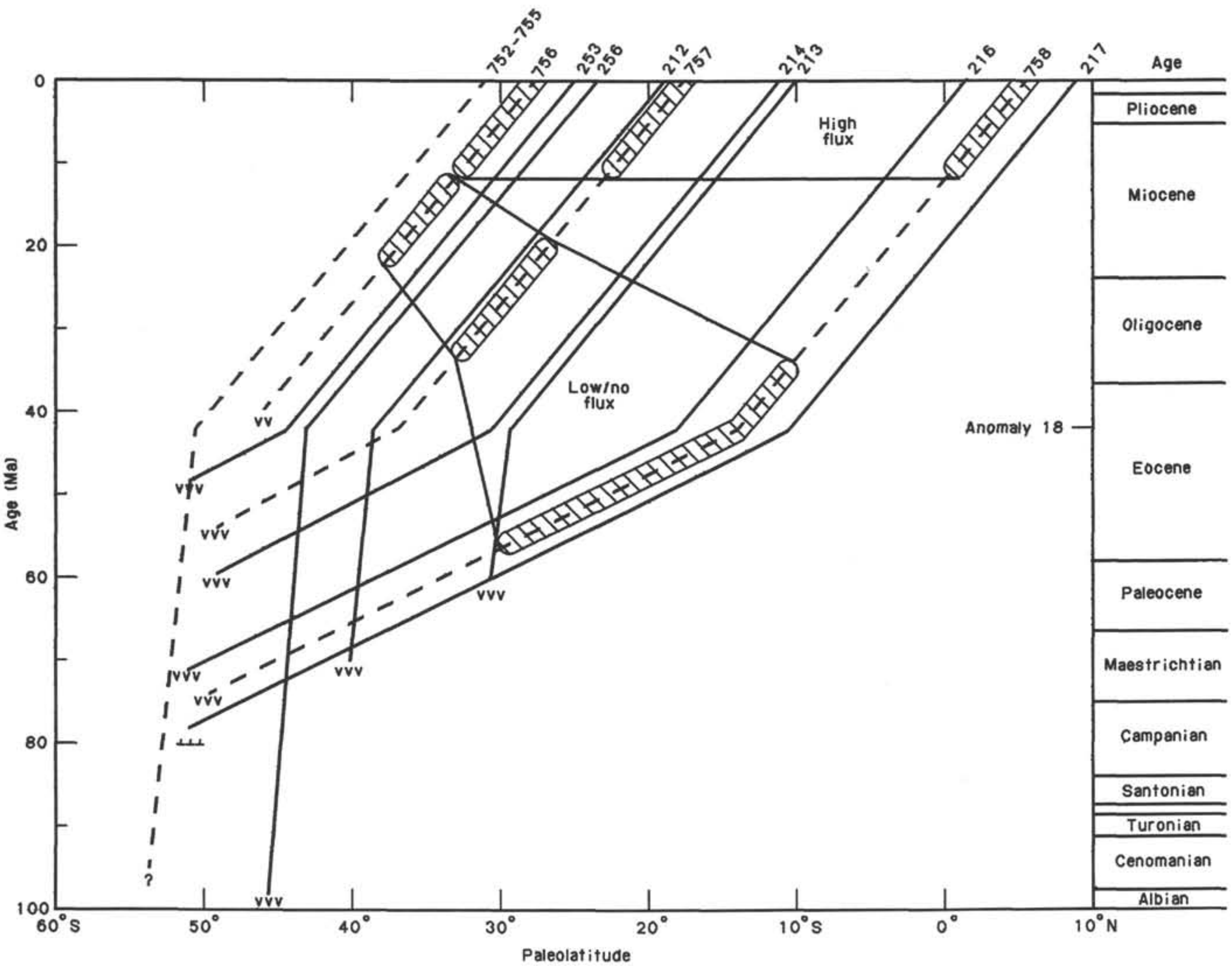

Figure 3. Regions of high and low flux on the Ninetyeast Ridge space-time backtrack diagram.

diffusion of the ashes is normally caused by bioturbation and can increase the thickness of the ashes by a maximum of 60% (Ruddiman and Glover, 1972). The basaltic glass is commonly altered to palagonite, clays (usually smectite), and chlorite. In most of these layers alteration of the glass to clay is less than 30%, though layers with more alteration were observed. At Site 758 the ashes comprise more than 10% of the sediment in the upper Campanian of Core 121-758A-41X, and their proportion increases steadily downcore. Clay becomes the dominant sedimentary component from Cores 121-758A-32X to 121-758A-48X. Most of the clay here is derived from the alteration of volcanogenic glass, as can be clearly seen in the smear slides as clay rims formed around the glass shards and in vesicles (see "Lithostratigraphy and Sedimentology" section, "Site 758" chapter).

Thick Ash Layers

Thick ash layers, composed of a series of smaller events, dominate the volcaniclastics discovered at Sites 757 and 758. The thick ash layers were first seen in Sections 121-757B-24X-3 and 121-758A-48R-1, from where they continue downhole through the remainder of the sedimentary section. They range from poorly indurated ashes to tuffs and grade in color from greenish gray (5G 5/1 and 5G 6/1) to very dark greenish gray (10GY 3/1 and 5GY 4/1) as the ash content increases to more than 85%. These layers are primarily basaltic in composition, although three silicic layers less than 10 cm thick and with sharp upper and lower contacts were observed in Section 121-758A-54X-4. These silicic layers resemble those found in Core 121-758A-1H and probably represent an eruptive episode of similar style. In the basaltic ash layers, as much as 30% to 50% of the glass has been altered to clay. Also altered are mineral fragments, particularly the plagioclase crystals, which are the most common mineral component. Shell fragments are common in the ash layers, forming a layer of ashy shell "hash" about 50 cm thick in Core 121-757B-25X.

The thick ash layers have two configurations:

1. Graded and cross-bedded, fine to coarse ashes.
2. Fine-grained ashes with accretionary lapilli.

Bedded ashes are present at both Sites 757 and 758. These are typically fine grained, with scattered coarse, graded layers. The fine-grained layers are rarely cross bedded and are not graded. They appear to be well-sorted ash deposits that settled through the water column and were reworked (Fig. 4). The coarse-grained layers are less than 50 cm thick and commonly have graded bedding. The layers with scoured basal contacts (Fig. 5) are thought to be turbidity flow deposits of ash that cas-

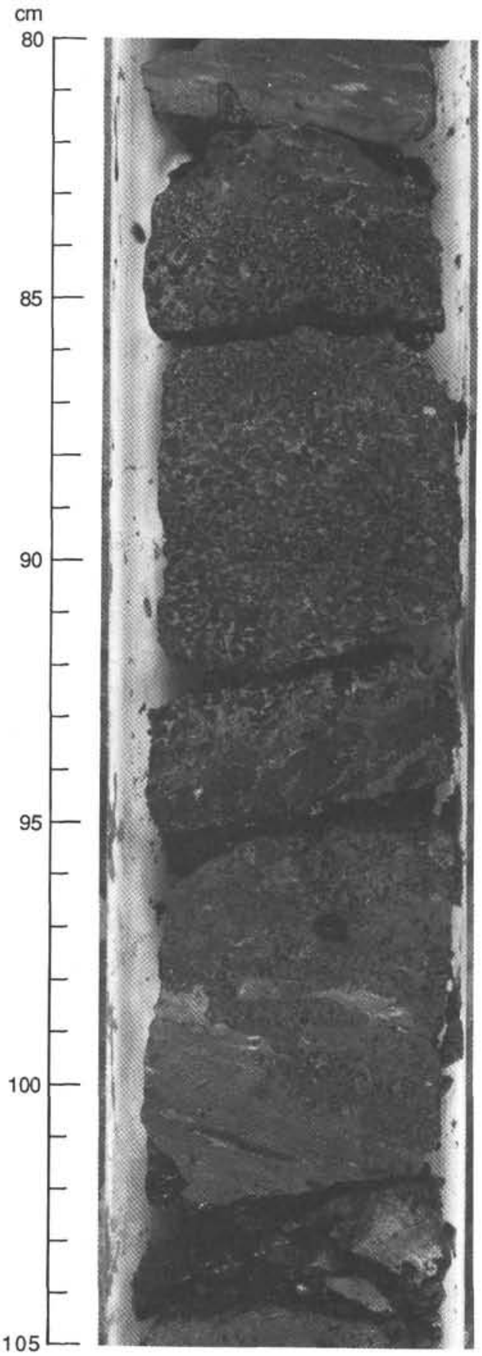

Figure 4. Coarse ash layer in Section 121-758A-54R-1, 80–105 cm. Graded bedding is visible in four discrete layers, and fine layering is visible in the fine-grained ash at the margins of the turbidity flows.

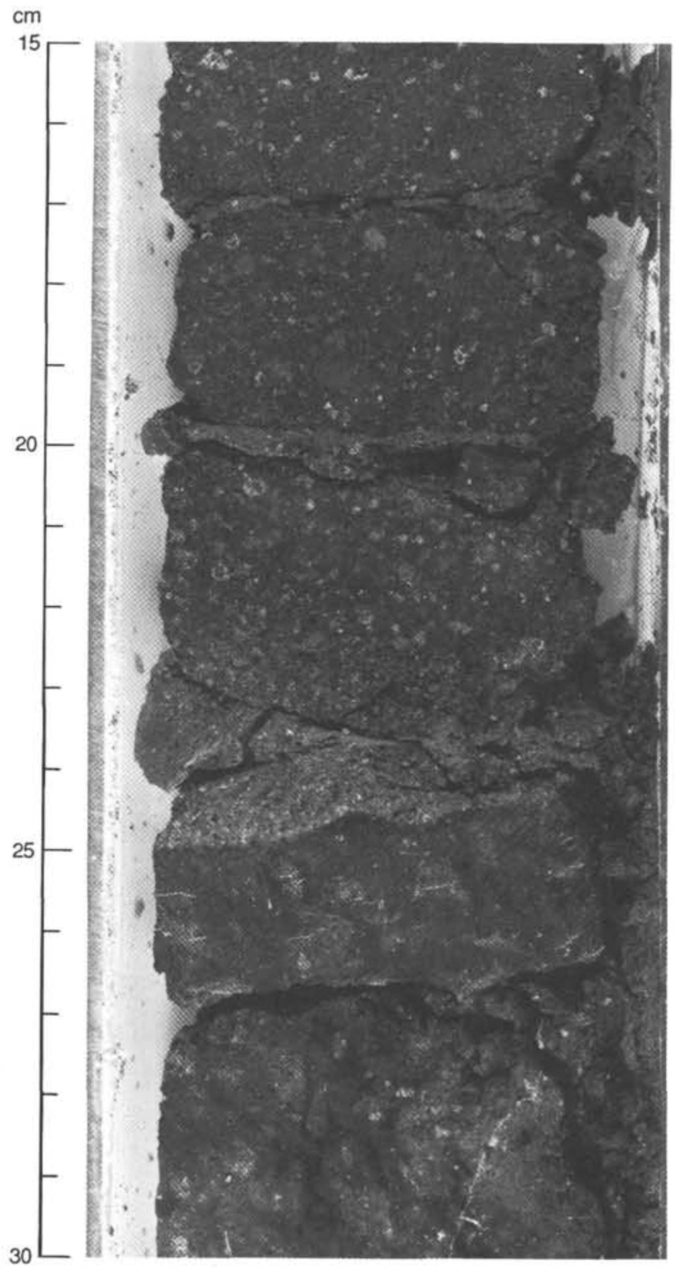

Figure 5. Coarse-grained ash layer with a scoured basal contact over a fine-grained layer in Section 121-757B-25X-2, 15–30 cm. Lapilli-size fragments are weakly graded in the coarse layer.

caded off of the slopes of the volcanic pile. Conversely, deposits without basal scouring could be ash falls that were thoroughly winnowed by settling in moderate currents. Similar deposits have been observed in hydroclastic tuffs from the Japan arc, and similar size distributions (i.e., the nearly total loss of fines) have been experimentally produced by dropping ash through a water column (Fiske, pers. comm., 1987).

Accretionary lapilli were observed only at Site 757. They first occur in Core 121-757B-26X, reach a peak of 20% volume in Core 121-757B-28X, and then gradually decline to their last occurrence in Core 121-757B-38X. The lapilli are 2 to 4 mm in size and form weak layers less than 10 cm thick (Fig. 6). They appear as greenish gray (5G 5/1) spheres and spheroids in a very dark grayish green (5G 2.5/2) matrix of fine- to sand-sized ash.

Accretionary lapilli are formed when water droplets pass through a dry eruptive column made of very fine glass shards. The droplets collect particles and act as nuclei to which the fine glass particles aggregate. Large plinian eruption clouds are needed to form lapilli, as well as a water source, which is typically raindrops for continental cases. Basaltic volcanism does not typically form plinian columns. However, magma-water interaction in shallow water could increase the explosivity of a basaltic eruption from vulcanian to surtseyan.

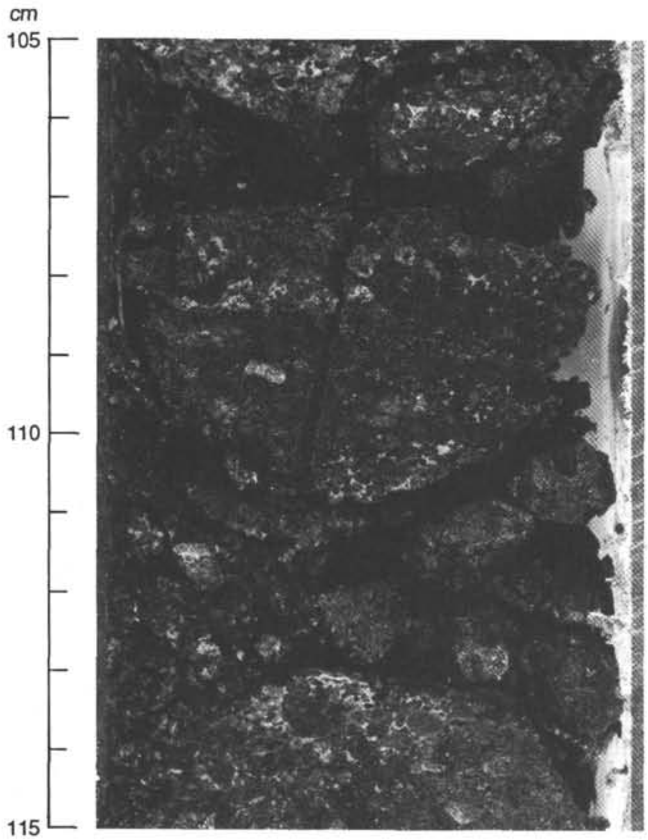

Figure 6. Accretionary lapilli forming weak layers in a fine-grained ash matrix in Section 121-757B-26X-2, 105–115 cm. Each lapillus is less than 4 mm in diameter, with shard size in the lapillus decreasing outward. Many lapilli are cemented with carbonate material.

Surtseyan eruptions, with lava-water interaction at sea level, form extremely large eruption columns and may create lapilli by a combination of the following three processes:

1. Abundant quantities of water and steam can provide the original water droplets to form lapilli nuclei.
2. Steam explosions are very high energy and produce eruption columns with large amounts of very fine-grained tephra.
3. Column collapse in these eruptions provides the mechanism to deposit the lapilli near the vent before they are disaggregated.

Accretionary lapilli occur only near the source vent (less than 10 km distance). Shell fragments and layers of shell hash were observed near and around the lapilli, indicating a shallow-water environment and thus confirming the possibility of surtseyan eruption.

Accretionary lapilli have been only rarely observed from hydroclastic eruptions, and they differ from their continental counterparts in that hydroclastic accretionary lapilli are vesicular. In thin section, the lapilli are devitrified, with clays filling vesicles throughout the lapilli. The grain size of the glass decreases outward in the lapillus. The lapilli on Ninetyeast Ridge appear to have been cemented together after deposition by carbonate material, and this could account for the good preservation of the layers.

Intercalated Ash Layers

The third type of ash layer is a small layer, less than 2 m thick, that occurs between lava flows in the lower part of Hole 758A. These layers are generally poorly recovered fragments or biscuits. The ashes are typically fine grained and fill irregularities in the tops of the basalt flows. Few contacts were recovered, but the upper contacts appear baked, with quench structures visible in the adjacent basalt flows. The lower contacts show increased alteration of the ash at the contact with the basalt. The alteration is primarily to smectite and chlorite. Ankerite, identified by X-ray diffraction, is a common white mineral that fills cracks in and near the contacts. Graded bedding, with scoured basal contacts, marks several small turbidity flows in these interbedded ash layers. These deposits cover the surfaces of several undersea basalt flows, and in turn have been buried by new flows. Burrowing was observed only in Section 121-758A-66R-1. These layers may be air-fall deposits because they are not graded and show bioturbation.

Conclusions

Tephra layers at Sites 757 and 758 have three distinctive phases of deposition. At both sites tephra was first deposited on submarine lava flows as air-fall settling through the water column with interspersed turbidity deposits of volcaniclastic or epiclastic material flowing off of the flanks of the volcanic pile.

At Site 757 the eruptive center was at or near sea level. The resultant magma-water interaction caused large surtseyan-type eruptions that created hydroclastic accretionary lapilli and thick fine-grained ash deposits. Subsidence followed, allowing for the deposition of the nannofossil oozes and the youngest ash layers.

At Site 758 turbidity flows and air falls persisted after the production of local lavas in relatively deep water had ceased. The ash layers could be the distal facies of large surtseyan or vulcanian eruptions. Ash deposition waned after the Campanian until Holocene time, when several large silicic air falls were emplaced. These ashes were erupted from large explosive events, thought to have occurred with the creation of the Indonesian arc. The most recent of these layers is tentatively correlated with the last large eruptive event at the Toba caldera.

IGNEOUS PETROLOGY

The origin of Ninetyeast Ridge, one of the longest linear topographic features on Earth, is not fully understood. This ridge is approximately 5000 km long and 200 km wide, with an estimated age ranging from 90 Ma at its northern end to 38 Ma at its southern end, where it is truncated by the middle Tertiary seafloor spreading of the Southeast Indian Ridge (Fig. 1). The origin of Ninetyeast Ridge is closely linked to the rapid northward motion of the Indian plate during the period from 90 to 53 Ma (Luyendyk, 1977). Based on radiometric and fossil age constraints, the ridge is believed to be part of the Indian plate. Ninetyeast Ridge is bounded on its eastern flank by a discontinuous, steep scarp (Sclater and Fisher, 1974), interpreted as a transform fault between the Indian plate and the Australian plate. The age of the last motion along this fault is not known, but major motion ceased when the Indian and Australian plates became coupled about 42 m.y. ago.

The present consensus is that Ninetyeast Ridge is related to magmatism overlying a mantle hot spot (e.g., Duncan, 1978; Peirce, 1978; Curray et al., 1982; Morgan, 1981; Royer and Sandwell, in press), but the exact geometry of Ninetyeast Ridge, the hot spot, and the contemporaneous plate boundaries is unclear. Specifically, how did the hot spot relate to the Indian-Antarctic spreading center? Was the hot spot located on the spreading axis (like Iceland) or was the hot spot off axis (like Galapagos or Hawaii)? And, very importantly, how does Ninetyeast Ridge relate to the Kerguelen-Heard Plateau, which contains two recently volcanically active islands, Kerguelen and Heard.

A hot-spot model for the Ninetyeast Ridge is consistent with several observations: (1) the composition of the Ninetyeast Ridge basalts is similar to that of basalts on some oceanic islands (e.g., Frey et al., 1977; Mahoney et al., 1983); (2) the paleomagnetic data indicate that the Ninetyeast Ridge basalts erupted at approximately 50°S (Cockerham et al., 1975; Peirce, 1978), which is in the vicinity of Kerguelen Island; (3) the similarity between the ages, increasing to the north, and subsidence rate of the ridge and the adjacent Indian plate indicates that Ninetyeast Ridge was constructed on the Indian plate (e.g., Sclater et al., 1973; Detrick et al., 1977).

The hot-spot model runs into serious difficulties when attempts are made to relate the hot spot to contemporaneous plate configurations. For example, much of the ridge was produced between 90 and 50 Ma, the period when the Indian plate was moving rapidly northward. Estimates for the closing rate between India and Asia vary, but Patriat and Achache (1984) suggested rates of 15–25 cm/yr for the period before anomaly 22 time (52 Ma). This is equivalent to 1500–2500 km in 10 m.y.

Although such rapid plate motions can explain the formation of linear features such as the Ninetyeast Ridge, there is an inherent problem; namely, the spreading center may also migrate and pass over an intraplate hot spot. Such an intersection was possible in the Indian Ocean system during the Cretaceous and Tertiary when India was migrating rapidly northward. Unless the Antarctic plate was migrating rapidly south, which would require twice the observed spreading rates, the spreading center would migrate northward rapidly. Most plate reconstructions (e.g., Morgan, 1981) require a near-stationary Antarctic plate during much of the Mesozoic and Cenozoic, so in this case the spreading ridge would migrate northward at its half rate of 8–13 cm/yr.

Because there is no linear feature of comparable length south of the Southeast Indian Ridge, the hot spot producing the Ninetyeast Ridge must have remained near the spreading axis that produced the adjacent Indian Ocean crust. To remain near such a rapidly migrating spreading axis is impossible unless (1) the spreading is strongly asymmetric or (2) there are southerly-directed ridge jumps that maintained the hot spot near the spreading axis (e.g., Sclater and Fisher, 1974; Peirce, 1978; Curray et al., 1982; Royer and Sandwell, in press).

Basement drilling by DSDP and ODP at seven sites on Ninetyeast Ridge demonstrated that the ridge is a volcanic structure. More than 1.5 millon cubic kilometers of lava was erupted over more than 40 m.y. This volume is similar to that forming the Kerguelen Plateau (Davies et al., in press) and is larger than the volume of the shield volcanoes forming the Hawaiian-Emperor Ridge (Bargar and Jackson, 1974). The principal problem is to understand the origin of this very large volcanic feature.

Our objective here is to use volcanologic, petrologic, and geochemical data from all of the DSDP and ODP ridge sites to constrain models for the origin and evolution of Ninetyeast Ridge. The data for basalts from ODP cores are from the "Igneous Petrology" sections of the chapters for Sites 756, 757, and 758.

Origin and Evolution of Ninetyeast Ridge

Volcanologic Constraints

An understanding of spatial and temporal variations in the volcanism that generated Ninetyeast Ridge is necessary to understand the origin of the ridge. Unfortunately, the number of basement sites relative to the size of the ridge is small, with an average of only one site per 650 km of linear ridge length. This would not be a problem if the different Ninetyeast Ridge sites are volcanologically similar. However, Leg 121 demonstrated that the lavas from each Ninetyeast Ridge site have significantly different compositions.

The relatively shallow basement penetration of 30–82 m at six of the sites and the 178-m basement penetration at Site 758 are unlikely to have sampled the early and main ridge-building phases of the Ninetyeast Ridge. This limitation must be recognized when using the recovered basalt to infer the origin of the ridge. Nevertheless, it is possible to draw some general conclusions from the volcanological data.

The topography of Ninetyeast Ridge suggests that this linear feature may have formed from eruptions from volcanic centers, with strongly localized activity generating the topographically higher parts of the ridge. The centers would naturally be areas where subaerial volcanism was more likely. In addition, such volcanic centers might well be characterized by the development of more evolved lavas, ferrobasalts and andesites, and an associated high-level hydrothermal system. Volcanism during the development of such volcanic centers would also result in a period of phreatic activity—either during the emergent or declining submergent phases. Such activity would generate thick, coarse-grained, proximal ash sections close to the volcanic centers. These characteristics of the volcanic centers are summarized in Table 2. Volcanism in areas between such centers would be characterized by the absence of evolved lavas, generally submarine effusive activity, low-temperature alteration in a submarine reducing environment, and the presence of distal ash layers.

Some of the DSDP/ODP Ninetyeast Ridge sites fit well into this theoretical framework. At both Sites 254 and 758, which are at opposite ends of Ninetyeast Ridge, there is no thick, coarse, proximal pyroclastic section overlying basement and no evidence of subaerial eruptions. The flows there are relatively magnesian in composition and the lavas are dominantly hyalopilitic in character. These features, and those of the overlying sediments, are compatible with submarine eruptions, perhaps in relatively deep water at Site 758, followed at both sites by low-temperature alteration in a reducing environment. In contrast, at Site 214, which is located near the crest of a local topographic high that was once an island on Ninetyeast Ridge, eruptions were clearly subaerial, the flows are more evolved in character, and a 100-m-thick clay, tuff, lapilli tuff, and lignite section overlies the lavas.

Classification of the other Ninetyeast Ridge sites is more ambiguous. For example, the flows at Site 756 were erupted in a subaerial environment, but a thick proximal ash section overlying the lavas is missing. The difficulty in classifying some sites is perhaps not surprising because all gradations between typical

Table 2. Characteristic features of volcanism at and between major volcanic centers on Ninetyeast Ridge.

Volcanic center activity	Between-center activity
Localization of activity leads to the formation of a well-defined volcanic center, with the local accumulation of basaltic lavas, and eventually to the eruption of subaerial flows.	Less frequent submarine eruptions, in a deep-water environment (pillow lavas and sheet flows).
Formation of magma chambers leads to the eruption of more "evolved" lavas, including ferroandesites, and sparse, more felsic compositions.	Mafic, Mg-rich flows dominate.
Localization of activity leads to an active hydrothermal system and higher temperature alteration of the lavas.	Alteration restricted to low-temperature smectite/calcite alteration in a reducing environment.
Thick deposits of coarse proximal ashes erupted in a neritic environment are dominant.	Bedded layers of finer, distal ashes intercalated in deep-water sediments or mafic flows. Ashes are derived from volcanic centers.

"volcanic center" locations and "between center" locations must exist.

An important geochemical result is that the ashes from Sites 758 have different incompatible element ratios than the underlying basalts (Fig. 31 of the "Site 758" chapter). The generally fine-grained, bedded nature of these ashes suggests that they are distal ashes, perhaps derived from a volcanic center tens of kilometers from the source of the Site 758 lava flows. The results suggest that the parental magma compositions in these two regions are significantly different. A comparable pattern of ash-basalt difference was observed at Site 757 (Fig. 25, "Site 757" chapter).

Another characteristic of Ninetyeast Ridge volcanism is that most of the sites are interpreted as having suffered relatively rapid subsidence during the waning stages of volcanism and/or during the subsequent few million years. Ash sequences, or ash-rich sediments, overlie the majority of the Ninetyeast Ridge basement sites, and these seem to characterize the post-extrusive phase. The last volcanic products may be distal ashes erupted from adjacent areas of phreatic volcanism. Upper Cretaceous to Eocene ash is a significant feature in the sedimentary pile at Broken Ridge (see "Tephra" section, "Broken Ridge Summary" chapter, this volume). This thick section of distal ashes developed because Broken Ridge remained close to the Kerguelen hot spot during that time (e.g., Figs. 7 and 17; Mutter and Cande, 1983).

Petrologic and Geochemical Constraints

Petrologic and geochemical data for lavas from DSDP and ODP Ninetyeast Ridge sites constrain two important aspects of the Ninetyeast Ridge volcanism:

1. How do lava compositions vary as a function of age from the extremes of ~38 Ma at Site 254 to ~80 Ma at Site 758?
2. How have lava compositions evolved with time at the individual sites on Ninetyeast Ridge?

In the following discussion, we use shipboard data for Leg 121 Sites 756, 757, and 758 plus literature data for DSDP Sites 214, 216, and 254 to address these questions and discuss the implications of the results.

Long-Term Geochemical Trends (38 to 80 m.y.)

Geochemical data for the Ninetyeast Ridge lavas of widely varying age may provide answers to the following questions:

1. Did a single mantle-source composition provide magmas for construction of the ridge or were two or more sources involved? In the latter case, what were the relative proportions of the sources and how did they change with time?
2. If an ocean island basalt source was involved, was this source similar to an intraplate hot-spot source, such as Hawaii, a ridge-centered source, such as Iceland, or an off-axis source, such as Réunion or Galapagos?
3. How similar are Ninetyeast Ridge lavas to lavas from the Kerguelen Archipelago?
4. Do Ninetyeast Ridge basalts have a Dupal geochemical signature (Dupre and Allègre, 1983; Hart, 1984; Sun and McDonough, in press); that is, do they have the anomalous geochemical signature that is characteristic of oceanic islands in the Southern Hemisphere from 20° to 50°S?
5. What was the role of a depleted mid-oceanic ridge basalt (MORB) source in creating Ninetyeast Ridge?

Lavas from Ninetyeast Ridge are dominantly tholeiitic basalts that range widely in SiO_2, FeO/MgO, and incompatible element content (e.g., Fig. 8). The shipboard chemical analyses provide precise and accurate data for the relatively immobile incompatible elements P, Y, Zr, and Nb. In fact, the quantity of the data for these elements obtained aboard ship during Leg 121 exceeds that from all previous studies of Ninetyeast Ridge basalts. Basement basalts from each site define significant intersite

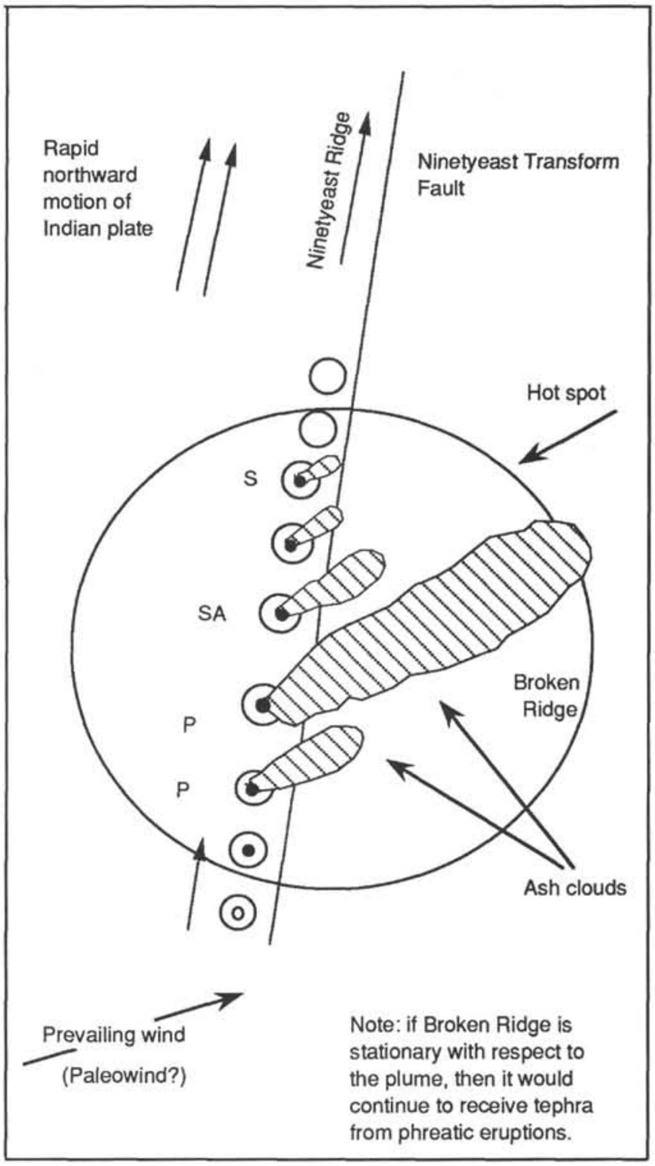

Figure 7. Schematic map of the southern Ninetyeast Ridge/Broken Ridge area during the Late Cretaceous-Paleocene illustrates a possible explanation for the longevity of the basaltic ash eruptions recorded at Broken Ridge (Sites 752 through 755). The Broken Ridge crust and the mantle plume associated with the Ninetyeast Ridge are assumed to have been stationary with respect to each other. As the Indian plate moves across the plume, it domes upward and is penetrated by hot-spot-related magmatism. The uplift brings the magmatic activity into the zone where phreatic (P) explosive volcanism can occur; as the volcanism becomes subaerial (SA) the volcano will be carried northward and further explosive activity will occur as the volcano subsides (S). Such a model may be necessary to explain the long time period during which basaltic ash was deposited on Broken Ridge (> 30 m.y.). The key to the model is the unusual, but not unlikely, juxtaposition of a hot spot and rapidly migrating lithosphere separated from stationary crust by a major transform fault system (the Ninetyeast Transform Fault). The spreading center was coincident with or south of the hot spot. Note that the predicted location of the hot spot provides a potential focus for the future rupture of Broken Ridge from the Kerguelen Plateau (Morgan, 1981).

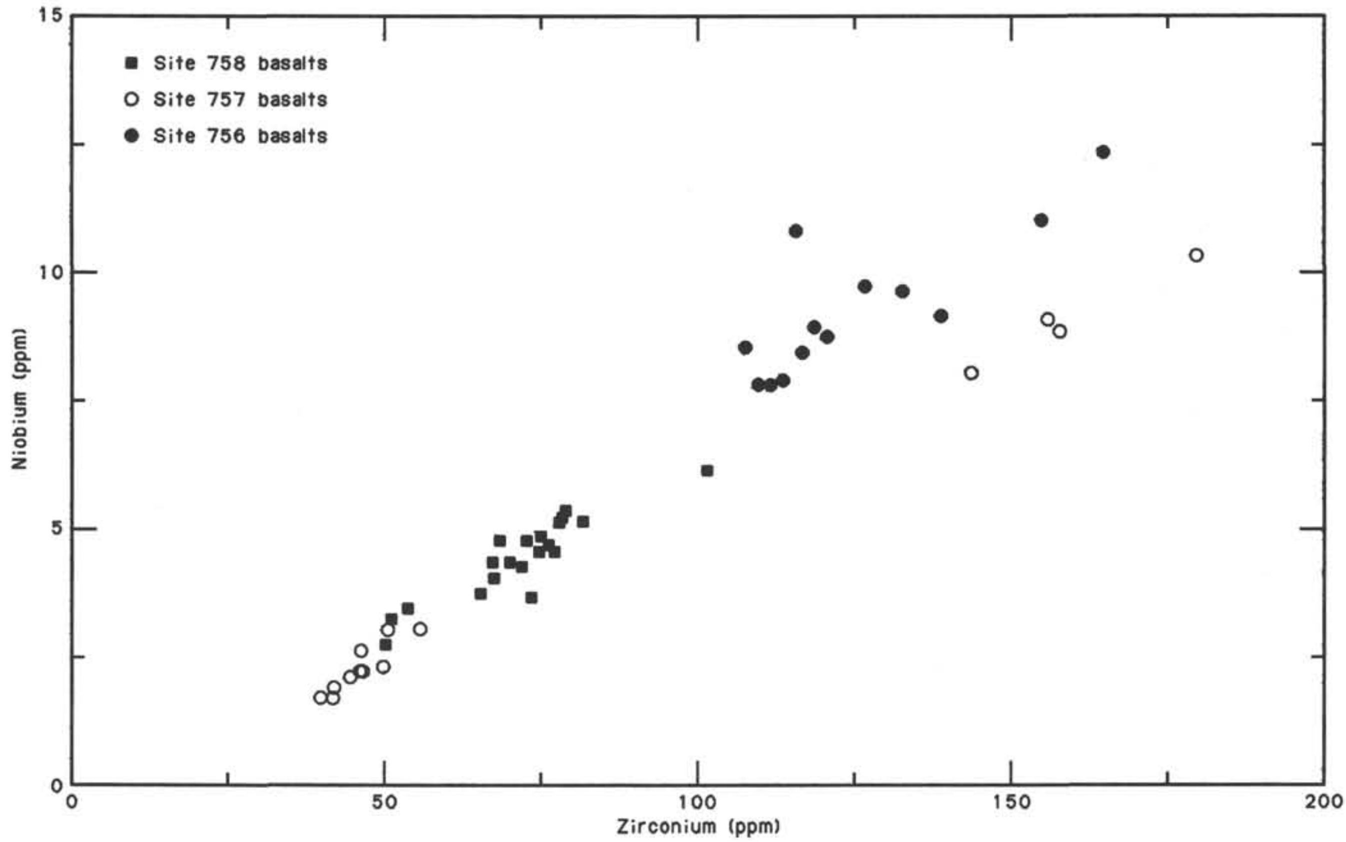

Figure 8. Abundances of Nb and Zr in basement basalts from Sites 756, 757, and 758. The data range by over a factor of three but form a nearly linear trend with little overlap among lavas from each site.

compositional differences (e.g., Figs. 9 and 10), but none is similar to incompatible element-depleted basalts formed at Indian Ocean spreading-ridge axes (i.e., MORB). However, the major element compositions of Ninetyeast Ridge basalts are similar to tholeiitic and transitional basalts erupted on some oceanic islands (e.g., Iceland and Galapagos; Frey et al., 1977).

The dominance of tholeiitic basalt on Ninetyeast Ridge is an important result because many oceanic islands and some hot-spot traces appear to be composed dominantly of alkalic basalt. Tholeiitic basalt is believed to form by extensive melting, and most major hot-spot-related volcanoes are composed dominantly of tholeiitic basalt (e.g., Hawaii, Iceland-Faeroes, Galapagos, and Réunion). Also, smaller islands astride ridge axes in the Southern Hemisphere, such as Ascension and Bouvet in the Atlantic Ocean and Amsterdam and St. Paul in the Indian Ocean, are composed of transitional to tholeiitic basalt. The large oceanic plateaus in the western Pacific (Mahoney, 1987) and the Kerguelen Plateau (Davies et al., in press; Schlich et al., 1988) are also composed primarily of tholeiitic basalt. In a recent summary of radiogenic isotopic data for basalts from the Pacific plateaus, Mahoney (1987) concluded that these plateaus formed from near ridge-axis hot spots because this tectonic setting is a plausible environment for voluminous volcanism, extensive melting, and mixing between MORB and ocean island basalt components (a characteristic of Ninetyeast Ridge lavas subsequently discussed in this chapter). In addition, this tectonic setting could account for the rapid subsidence of Ninetyeast Ridge and the accompanying accumulation of ash that formed in a shallow-marine environment (Fig. 7).

Radiogenic isotope ratios and incompatible element abundance ratios of basalts can provide constraints on mantle compositions. Isotopic data for Ninetyeast Ridge Leg 121 basalts require shorebased analyses. Currently, there are no combined sets of Sr, Nd, and Pb isotopic data for the Ninetyeast Ridge lavas. However, the existing isotopic data (Figs. 11 and 12) show significant Sr and Nd isotopic differences between ferrobasalts from Ninetyeast Ridge Sites 214 and 216 and are sufficient to show that lavas from DSDP Sites 214, 216, 253, and 254 are unlike MORB or lavas from St. Paul and Amsterdam islands. However, Nd isotopic ratios of lavas from Ninetyeast Ridge are similar to Nd isotopic ratios of the older tholeiitic and transitional basalts from the Kerguelen Archipelago (Fig. 10; White and Hofmann, 1982; Weis et al., 1987b). The two Pb isotopic analyses of Ninetyeast Ridge lavas (Dupre and Allègre, 1983) are also similar to those of Kerguelen Island and Kerguelen Plateau lavas (Fig. 12; Weis et al., 1987a, 1987b). If the range of Nd and Sr isotopic ratios observed within the different basaltic series of Kerguelen reflect different proportions of mixing between a depleted, MORB-type component and a very enriched, ocean island basalt-type component (Weis et al., 1987b), the Ninetyeast Ridge basalts may also have resulted from mixing of these components. Obviously, an evaluation of this mixing model requires more isotopic data for lavas from each of the Ninetyeast Ridge sites.

The numerous data for incompatible elements, largely from shipboard studies, establish that there are significant intersite geochemical variations among basement basalts (Figs. 8–10). Do these differences in trace element abundance reflect derivation from compositionally different mantle sources or do they result from complex post-melting processes? Radiogenic isotopic data are needed to address this question. In oceanic basalts, however, variations in Zr/Nb are usually accompanied by

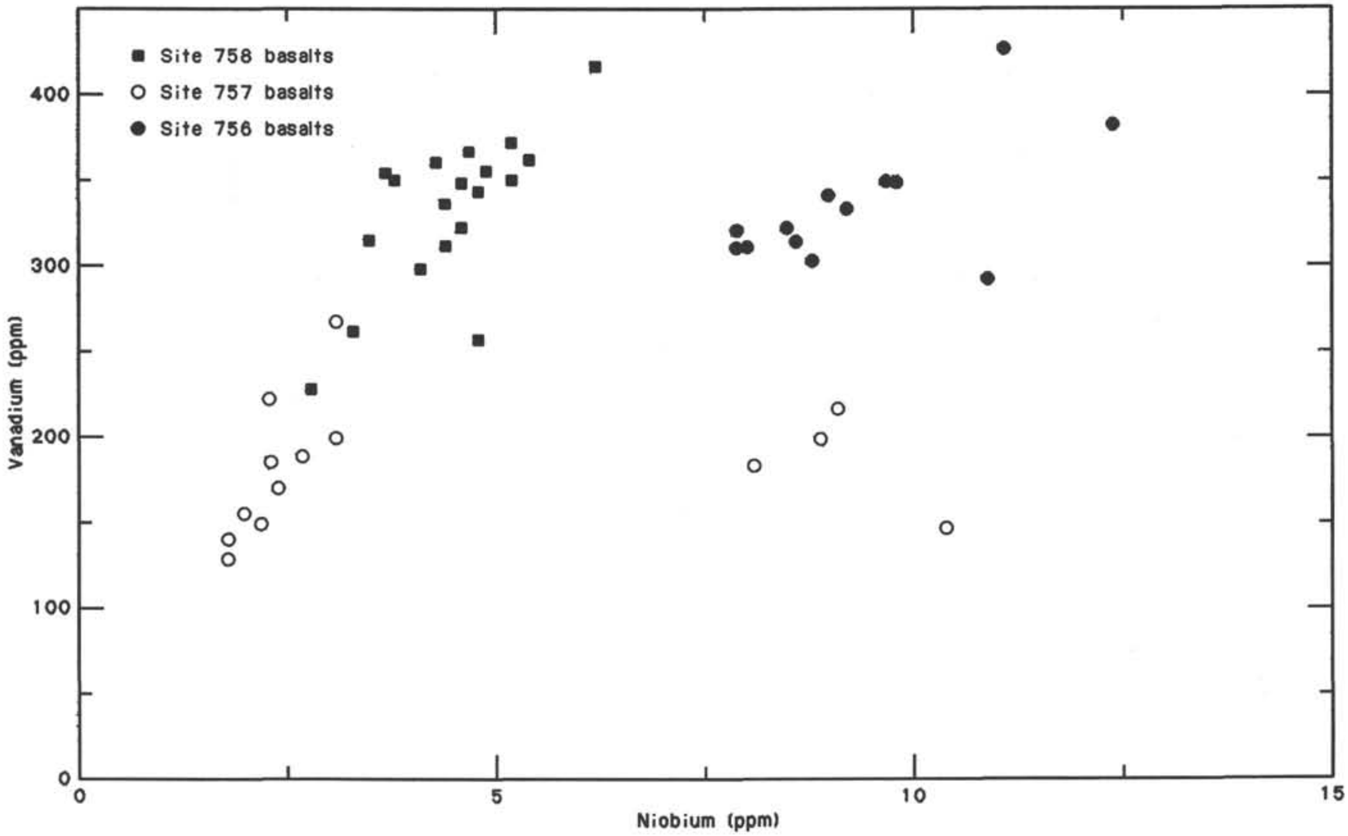

Figure 9. Abundances of V and Nb in basement basalts from Sites 756, 757, and 758. Each site defines a distinct field.

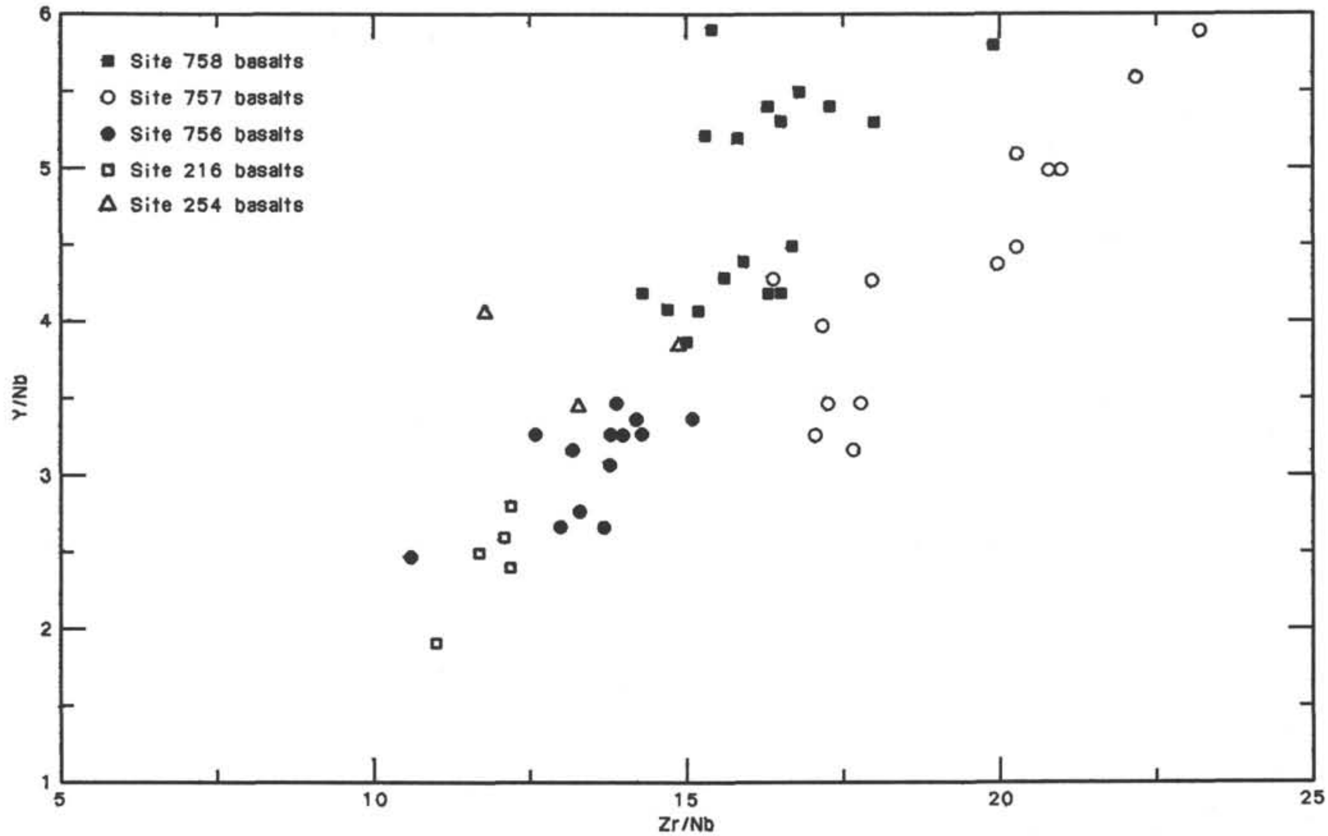

Figure 10. Y/Nb vs. Zr/Nb for Ninetyeast Ridge lavas. Each of the sites defines a different field.

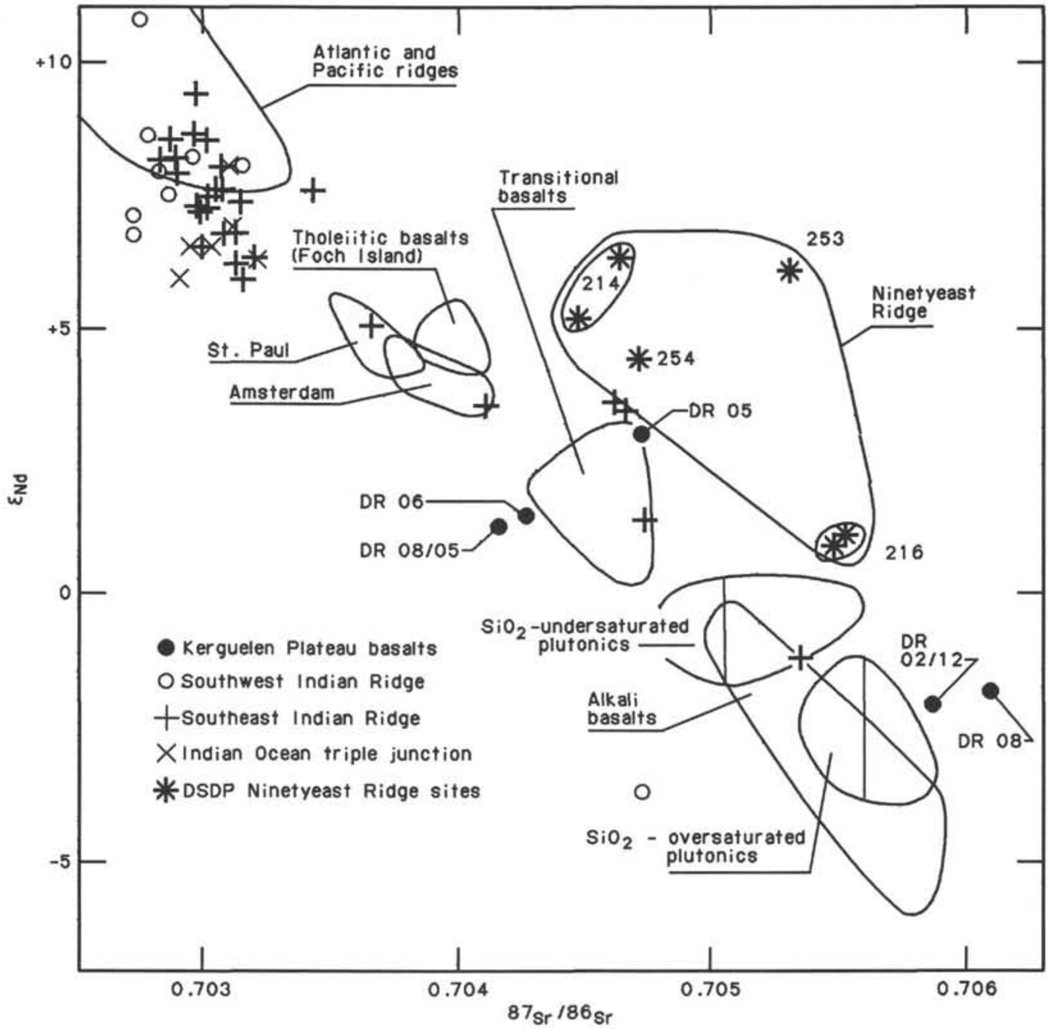

Figure 11. $^{143}Nd/^{144}Nd$ vs. $^{87}Sr/^{86}Sr$ ratios in lavas from Ninetyeast Ridge (Subbarao et al., 1977; Mahoney et al., 1983), Kerguelen Archipelago (Weis et al., 1987b), and Kerguelen Plateau (MD-48 dredge samples; Weis et al., 1987b, in press). DR = dredge sample. The Kerguelen basalt series define three separate fields—tholeiitic series ($^{87}Sr/^{86}Sr$ about 0.704), transitional series ($^{87}Sr/^{86}Sr < 0.7048$), and alkaline series ($^{87}Sr/^{86}Sr > 0.7050$ and up to 0.706) —which also correspond to a clear limit in ϵ_{Nd} values at 0. These geochemical differences correspond to a geodynamical evolution of the archipelago; when it was still close to the Southeast Indian Ridge 40 m.y. ago, the magmatism was tholeiitic to transitional and evolved toward alkaline magmatism with more enriched characteristics as the islands moved away from the ridge toward their present-day intraplate position. Data for the Indian MORB from Hamelin and Allègre (1985) and Hamelin et al. (1986).

isotopic variations (e.g., LeRoex et al., 1983, 1987). Therefore, we tentatively accept that Zr/Nb variations in tholeiitic basalts reflect source differences.

Variations in Y/Nb and Zr/Nb ratios in the Ninetyeast Ridge lavas show that these lavas do not overlap with MORB or Kerguelen Island lavas (Fig. 13). However, the nearly linear trend in Figure 13 provides evidence for mixing between MORB and enriched components similar to those represented in the Kerguelen lavas. The scatter from a straight line in Figure 13 may reflect heterogeneity in the MORB and ocean island basalt end-member components, the presence of other mantle components, or second-order variations caused by crustal processes such as crystal-melt fractionation, magma mixing, and assimilation.

Temporal compositional variations on a time scale of several millon years could provide constraints on the mixing process. For example, the proportion of MORB and ocean island basalt components should depend upon the distance between the hot spot and a spreading center. When a young spreading center overrides, or is near, the hot spot, a large MORB contribution is expected. Another important factor is possible episodic behavior of hot-spot plumes (e.g., Schilling and Noe-Nygaard, 1974), in which case instead of a hot-spot trace being formed from a continuous ascending diapir the trace may be fed by a series of discrete ascending blobs. In the latter case, the MORB/ocean island basalt mixing ratio changes significantly as a function of time. It is also possible that the hot-spot source remained stationary for long time periods relative to a spreading axis. If the hot spot was always near the spreading ridge, then a continuous hot-spot trace may be created rather than a series of isolated volcanic complexes (Vogt, 1974).

With the present data base we discern no systematic long-term variations in geochemistry along Ninetyeast Ridge. This conclusion must be tempered by the realization that only a very small part of the volcanic structure has been sampled. Nevertheless, several other long-lived hot-spot traces have retained their distinctive geochemical features for long time periods of 20 to

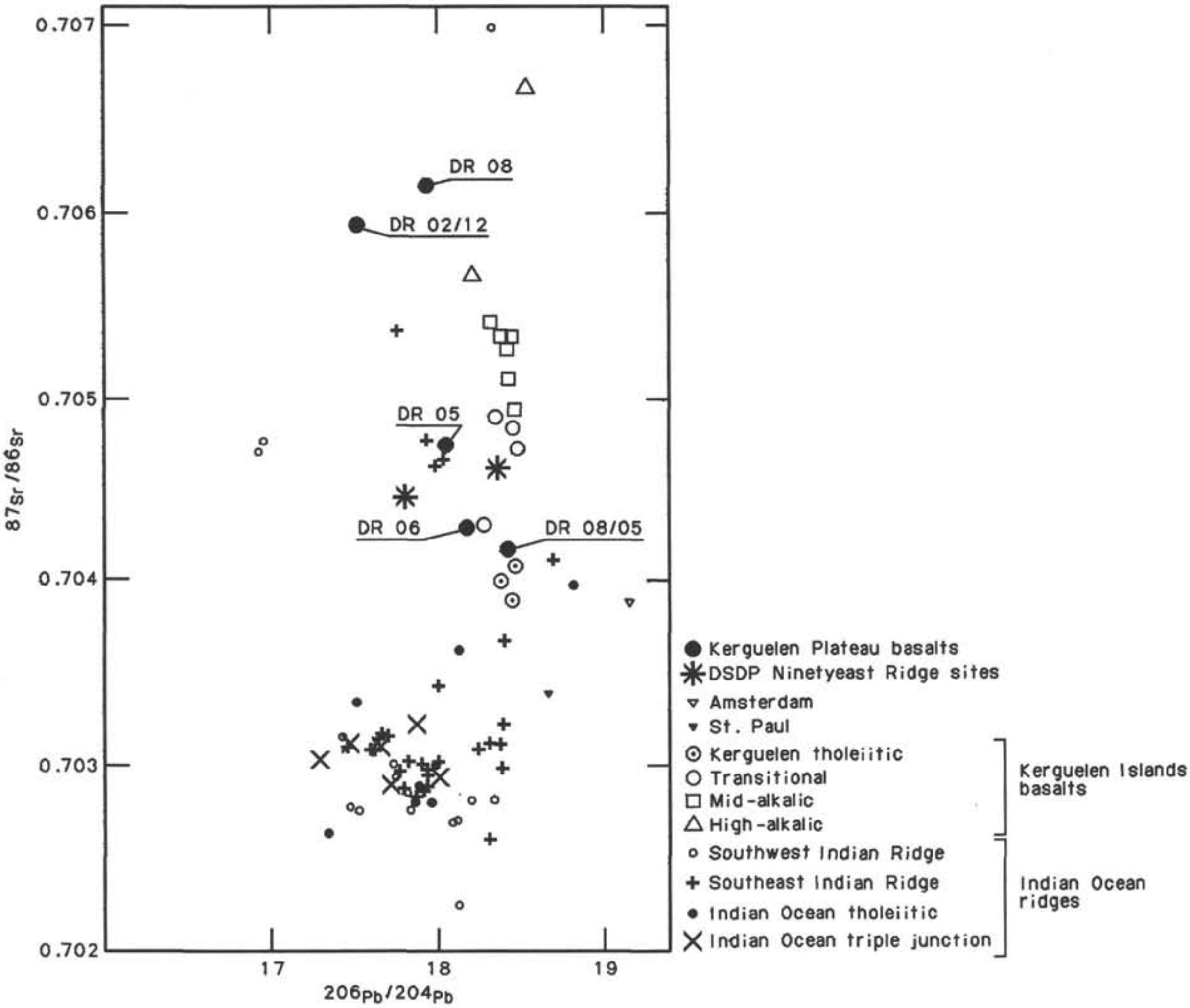

Figure 12. $^{87}Sr/^{86}Sr$ vs. $^{206}Pb/^{204}Pb$, with data for only two Ninetyeast Ridge lavas. DR = dredge sample. These two points are closest to the Kerguelen field and distinct from the fields for MORB and Amsterdam and St. Paul islands. Data sources as in Figure 11.

80 m.y.—for example, Hawaii (Frey and Roden, 1987; Stille et al., 1987), New England seamounts (Taras and Hart, 1987), and the Louisville Ridge (Cheng et al., 1987). Throughout the history of Ninetyeast Ridge, the erupted lavas may have been mixtures of components derived from a MORB source and an enriched, ocean island basalt source similar to what produced the Kerguelen Island magmas. Because basalts from the Kerguelen Archipelago have very distinctive radiogenic isotopic ratios (e.g., Weis et al., 1987b), isotopic analyses of the Leg 121 basalts will provide a sensitive test of this hypothesis.

Short-Term (~1 m.y.) Geochemical Trends—Compositional Variations at Individual Sites

A knowledge of geochemical variations at individual sites is needed to understand intersite geochemical differences. Moreover, the waning stages of hot-spot volcanism may define geochemical trends that provide information about mantle sources and crustal magma reservoirs. For example, at Hawaiian volcanoes—the most thoroughly studied volcanoes that form a long, linear hot-spot trace—there are major changes in volcanism as a volcano moves off the hot spot (e.g., Chen and Frey, 1985; Frey et al., in press). Lava-production rates decrease rapidly (see Fig. 11 in the "Leg 121 Background and Objectives" chapter, this volume), and there is a change from tholeiitic to alkalic lavas, presumably reflecting a decrease in the degree of melting. Because of infrequent replenishment from the mantle, crustal magma chambers become isolated, which enables extensive crystal fractionation of basaltic magma to form evolved, MgO-poor residual melts. As a result, most Hawaiian volcanoes are covered by a thin (10- to 1000-m-thick) veneer of alkalic and evolved lavas (see Fig. 12 in the "Leg 121 Background and Objectives" chapter). In addition, there is a systematic change in radiogenic isotopic ratios, with the youngest alkalic lavas having MORB-like isotopic ratios (e.g., Frey and Roden, 1987; Feigenson, 1986).

If similar processes occurred during the formation of Ninetyeast Ridge, the shallow basement penetration of DSDP and ODP drilling may record these changes in lava composition. There is strong evidence for isolated magma chambers at Sites 214 and 216, where ferrobasalts ($FeO^*/MgO > 2$) were recovered along with overlying oceanic andesites at Site 214 (Thompson et al., 1974). The plagioclase-rich lavas at Site 757 also provide evidence for extensive crystal-melt segregation within the crust. Moreover, none of the recovered Ninetyeast Ridge basalts has compositions in equilibrium with forsterite-rich ($Fo_{\sim 88-90}$) upper mantle olivine; either all the recovered Ninetyeast Ridge lavas had an extensive history of crystal-melt segregation in the crust or the Mg/Fe ratio in the mantle source of hot-spot volcanoes may be variable (Langmuir and Hanson, 1980).

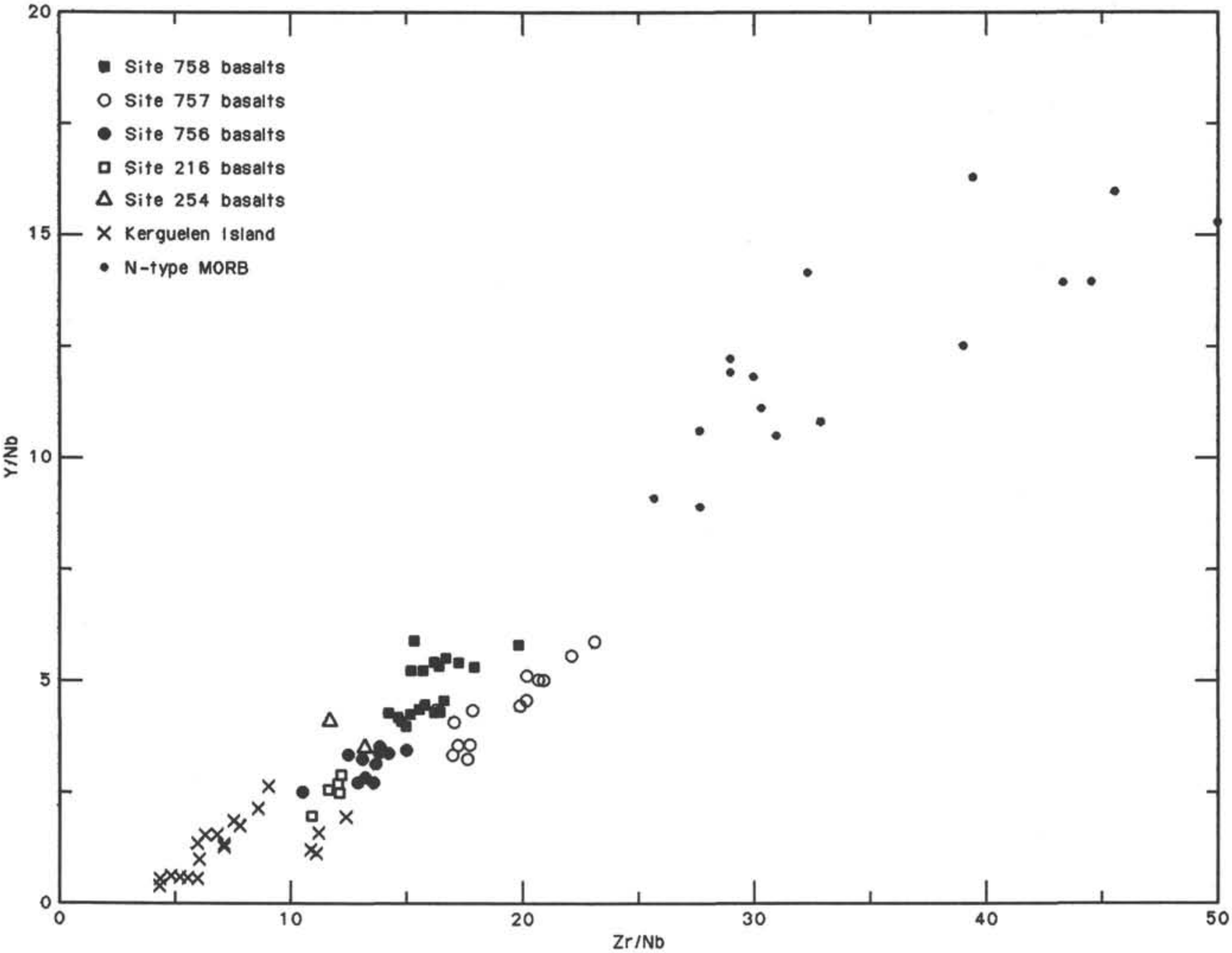

Figure 13. Y/Nb vs. Zr/Nb on a larger scale than Figure 10, showing that the variation among Ninetyeast Ridge lavas lies on a mixing trend between MORB and Kerguelen Archipelago lavas. Data sources from Price et al. (1986), Saunders (1983), Bougault et al. (1979), and M. Storey and A. D. Saunders (unpubl. data).

The only evidence for a change to alkalic volcanism as the Ninetyeast Ridge volcanoes aged is at Site 756, where the youngest lavas are transitional between tholeiitic and alkalic lavas. At Sites 214 and 256, the uppermost lavas are most enriched in incompatible elements, whereas at Sites 216 and 757 the lowermost lavas are relatively enriched in incompatible elements (Fig. 14). At Sites 253 and 254, thin (<2-m-thick) flows within the ash-rich units above basement are more evolved (lower MgO and higher incompatible element contents) than the underlying basement basalts.

Conclusions

1. Each drill site on Ninetyeast Ridge has provided important new information about the ridge. The first-order result is the systematic increase in basement age from south to north, which is consistent with a hot-spot model for the origin of Ninetyeast Ridge.

2. Important geochemical and petrologic results are that the lavas at each site have distinctive characteristics. For example, lavas from Sites 214 and 216 provide evidence for an extensive crustal history that enabled high degrees of fractional crystallization to develop ferrobasalts and oceanic andesites. Surprisingly, lavas from the Leg 121 sites did not recover similar highly evolved lavas. However, at Leg 121 Sites 757 and 758, there is clear evidence for plagioclase fractionation, even within individual flows.

3. Despite the intersite differences, the most important geochemical result is the broad similarity of the lavas from all of the Ninetyeast Ridge sites. Literature data for lavas from the DSDP sites showed that the ridge was constructed of tholeiitic basalt with trace element abundance characteristics similar to those of ocean island basalt. The Leg 121 results confirm the dominance of tholeiitic basalt, but the extensive trace element abundance data obtained aboard ship show that these Ninetyeast Ridge basalts have geochemical characteristics intermediate between MORB and ocean island basalt. In particular, Ninetyeast Ridge basalts have incompatible trace element abundance ratios on mixing trends between MORB and an ocean island basalt component represented by transitional basalts from the Kerguelen Archipelago (Fig. 13). Limited isotopic data for lavas from the DSDP sites show that the Ninetyeast Ridge lavas have radiogenic isotope ratios that most closely overlap the less-enriched portion of the isotopic field defined by the Kerguelen lavas (Fig. 11). Different Sr and Nd isotopic ratios at each site

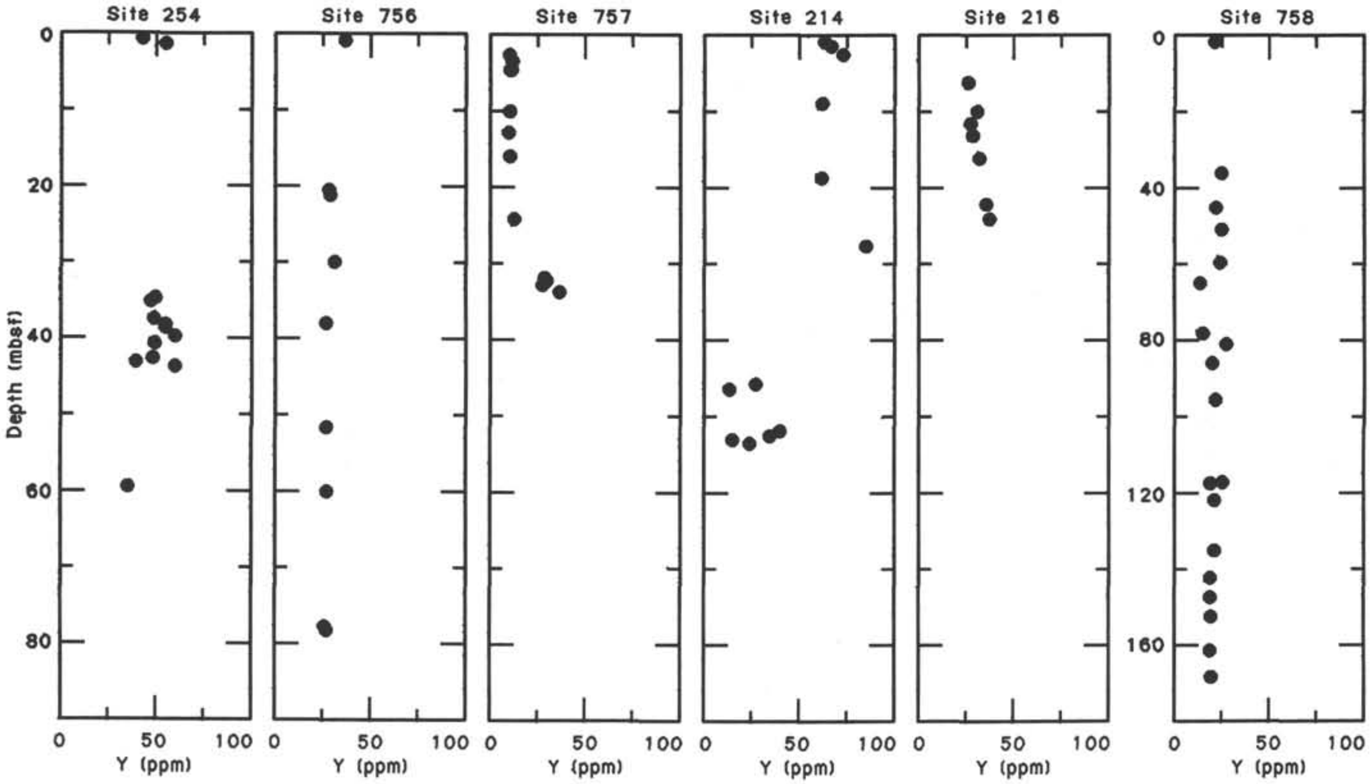

Figure 14. Abundances of Y as a function of stratigraphic level (age) in basalts from each site on Ninetyeast Ridge.

(e.g., Sites 214 and 216 in Fig. 11) are consistent with mixing of an MORB component with an enriched ocean island basalt component similar to that on Kerguelen.

4. Another characteristic of six of the seven Ninetyeast Ridge sites is the high abundance of basaltic ash overlying the basement lava flows. This is a unique feature of Ninetyeast Ridge relative to other hot-spot volcanoes. These ashes formed in shallow marine environments as subaerial volcanic centers emerged and subsided. Distal ashes from these volcanic centers cover much of Ninetyeast Ridge, and they were also found on Broken Ridge (Fig. 7). Apparently, Ninetyeast Ridge was constructed by discrete, subaerial volcanic centers. Between the volcanic centers, volcanic activity was limited to deep-water pillow and sheet flows, as recovered at Site 758. At any time during the history of the Ninetyeast Ridge, these different types of volcanic activity were occurring simultaneously on different parts of the ridge; however, at the locations of volcanic centers on the ridge there was a succession from deep-water submarine flows to phreatic eruptions to subaerial flows followed by a second phase of phreatic eruptions as the mature volcano subsided and moved north away from the hot spot (Fig. 15).

5. These conclusions imply that the hot spot was located near a spreading-ridge axis, which is consistent with the dominance of tholeiitic basalt on Ninetyeast Ridge and the mixing trends with an MORB component. The limited radiogenic isotopic data for DSDP lavas are consistent with an ocean island basalt source similar to that represented in the Kerguelen lavas. Isotopic analyses of Leg 121 lavas will provide a sensitive test of the mixing model and the relationship to the Kerguelen hot spot.

Proposed Future Research

Despite the increased understanding of Ninetyeast Ridge developing from ODP Leg 121, there are several important aspects of the ridge that need to be studied in order to fully understand its origin and evolution.

1. Technically feasible drilling at judiciously selected sites involving 300 to 500 m of basalt penetration could recover a significant proportion of the volcanic structure. The drilling targets should be possible volcanic centers as well as regions between these centers. A particularly interesting site is Osborne Knoll, a major unexplained bathymetric feature of the ridge.

2. Detailed side-scan sonar mapping of the ridge. The volcanic and tectonic structure of the ridge needs to be determined in detail at several locations.

3. Models for Ninetyeast Ridge proposed by Duncan (1978) and Curray et al. (1982) require that parts of the ridge have significantly different ages than the Indian plate to the west. These models can be tested by better definition of seafloor ages on and adjacent to Ninetyeast Ridge. For example, Royer and Sandwell (in press) proposed a southerly jump in the spreading-ridge axis of several hundred kilometers. All ridge-jump models require sections of Ninetyeast Ridge to be younger than the Indian plate to the west. Of course, the difference in ages depends upon the distance of the spreading-axis jump.

GEOCHEMISTRY

The chemical and isotopic compositions of pore fluids from deep sea drilling cores are very useful in evaluating the extent to which the oceanic crust undergoes alteration after it leaves the vicinity of the mid-ocean ridge. These compositions are also very useful in understanding fluid flow both in the basaltic basement and in the sediments, especially at very slow advection rates where heatflow anomalies may not reveal the patterns of fluid flow. Chemical and isotopic changes in the pore fluids—particularly changes in calcium ion concentrations and oxygen isotope ratios—are caused by the alteration of volcanic material to clay minerals, commonly smectites, and zeolites.

The Indian Ocean is an area where very large chemical and isotopic changes have been observed in pore fluids. The largest calcium ion changes within a sediment sequence were observed on Ninetyeast Ridge (Lawrence and Gieskes, 1981). The elevated

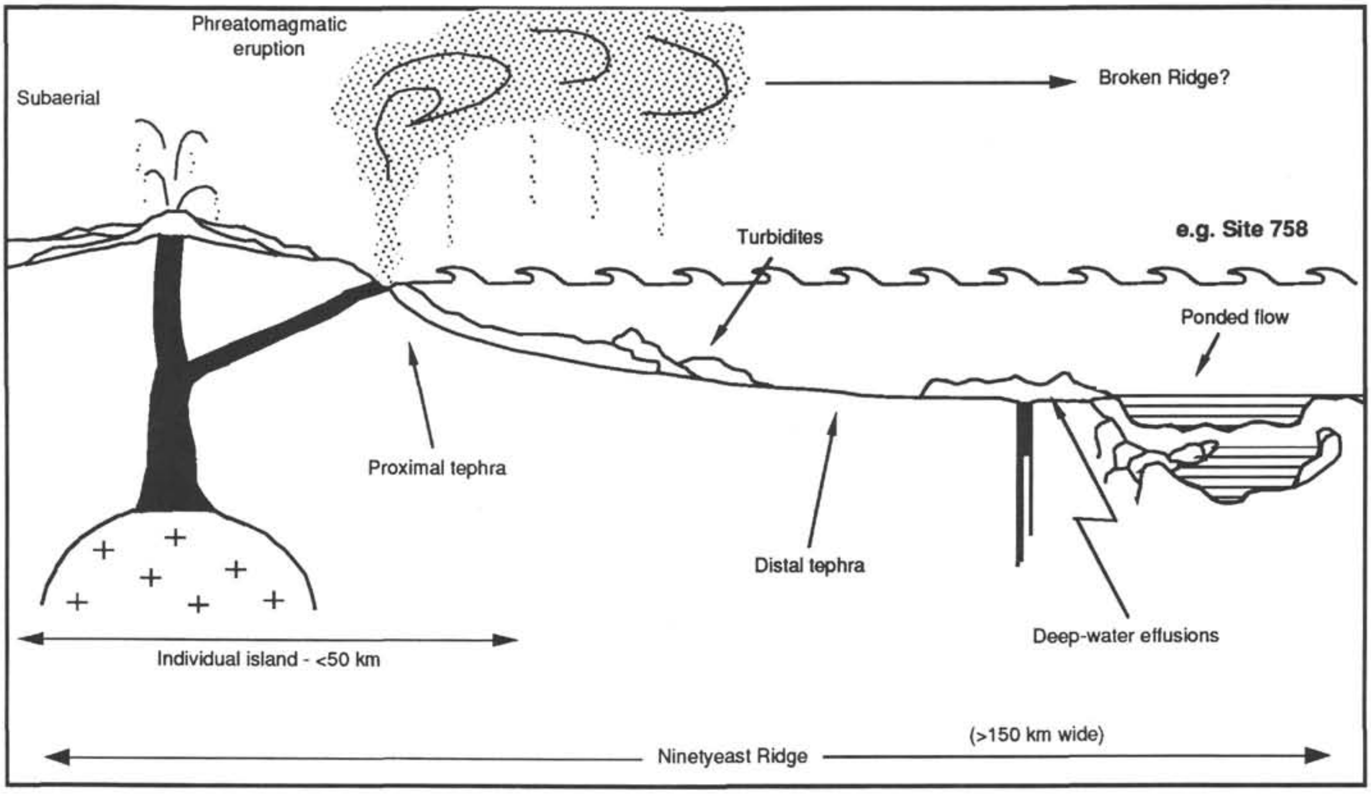

Figure 15. Schematic section across part of the Ninetyeast Ridge above the putative mantle hot spot, illustrating a possible scenario for the different volcanic facies observed from Leg 121 drilling. Note that the orientation of the section has been deliberately omitted. As illustrated on this figure, the ridge may comprise subaerial, phreatic, and deep-water eruptions at any one time. In this case the section can have any orientation, including east-west. At a specific location on Ninetyeast Ridge, a segment of crust migrating onto the hot spot may erupt submarine lavas before being uplifted through a phreatic stage and finally becoming subaerial. The volcano will then gradually subside as it is carried off the hot spot. For this scenario, the diagram can be considered as a north-south section along the ridge. Similar arguments can be made if Ninetyeast Ridge was produced on a spreading axis.

topography and extensive volcanism in the past created an ideal environment for basalt and ash alteration. Therefore, Ninetyeast Ridge represents an excellent location to find chemical anomalies in pore fluids and use them to understand patterns of alteration and fluid flow. For more detail see the "Inorganic Geochemistry" section of the "Site 756" chapter.

The magnitude and variability of chemical and isotopic gradients are useful in understanding the concentration of volcanic material in the sediments and the structure of the crust. The magnitude of the pore-water chemical vs. depth gradients is a function of the quantity and rate of alteration of volcanic material. The extent to which the crust is isolated from seawater is also important. The variability of the gradients in space is a function of the structure of the basement and sediment cover. This structure controls fluid transport in the crust and the access of deep ocean water to the crust.

Ninetyeast Ridge has a highly complex and variable structure. Some systematic changes roughly comparable to those exhibited by ocean crust as a function of distance from the ridge axis are found from south to north along the ridge. Ninetyeast Ridge becomes deeper and more heavily sedimented to the north. Its depth profile appears to subside at similar rates to normal oceanic crust (Detrick et al., 1977), indicating that the heat flow is less to the north. Therefore, some of the features of chemical change exhibited from south to north in the pore fluids in the sediments overlying Ninetyeast Ridge may be similar to those found in ocean sediments at progressively greater distances from a mid-ocean ridge.

Discussion

The most useful parameter to examine in comparing alteration and fluid flow patterns along Ninetyeast Ridge is the calcium ion concentration of the pore fluids (Fig. 16). Two major differences can be seen in the patterns of the calcium ion profiles with depth from site to site. First, the increase in calcium ion concentration with depth, the calcium gradient, is very different from site to site. Second, the calcium gradients from hole to hole are more variable at some sites. The highest gradient and the highest absolute calcium ion concentration in the pore fluids were found at Site 757. The very high values are caused by the extensive degree of alteration of the thick ash sequence (see "Inorganic Geochemistry" section, "Site 757" chapter). At the other two sites the amount of ash is much lower. At Site 756 ash was found only lightly dispersed in the carbonate sediment cover. Because the ash content of the sediments is low, most of the calcium signal probably results from alteration of the basaltic basement. At Site 758 the ash layer is less than half the thickness of that at Site 757. In addition, the ash has had a longer time to have altered at Site 758 because of its greater age. A fuller evaluation of the actual amount of alteration of volcanic material that has taken place at each of the sites will be better defined when oxygen isotope analyses of the pore fluids are completed on shore (see Lawrence and Gieskes, 1981).

The other major observation in the pore-water data from Ninetyeast Ridge is that the younger the basement age and the thinner the sediment cover, the bigger the differences in calcium

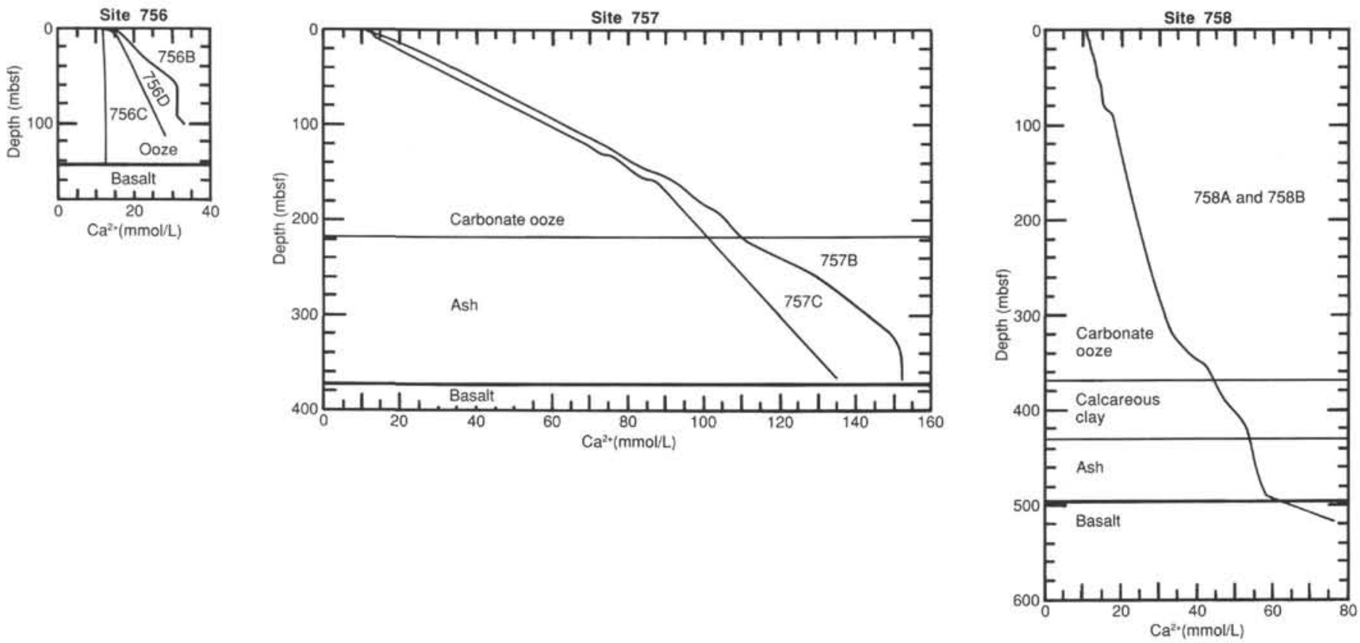

Figure 16. Calcium ion concentrations of the pore waters from Sites 756, 757, and 758 plotted as a function of depth for each hole. The major lithologies are given for each site.

ion profiles from hole to hole at any given site. At Site 756, the three drilled holes are spaced 100 m from each other in a nearly straight line (see "Operations" section, "Site 756" chapter). Large differences in the calcium ion gradient are observed over these short distances. There are two possible explanations for this. One is that because of the very rough topography in the vicinity of Site 756, seawater may have greater access to some parts of the basement than others via faults. The parts of the basement more isolated from seawater would act like a closed system and thereby develop higher concentrations of calcium. In this interpretation the basement is successively a more open system progressing from Holes 756B to 756D to 756C. The calcium profiles seen in the sediments represent diffusion of the calcium signal from the basement to the seafloor above. Because this signal varies in the basement it also varies in the sediments overlying the basement.

The other interpretation is that a convection system that includes both the basement and the sediments exists at Site 756. Hole 756C represents a downwelling zone, and Holes 756D and 756B are near the center of the cell where net-advection rates are low. Farther along in the direction from Holes 756C to 756D to 756B a different profile would be expected, with very high calcium concentrations very near the sediment/water interface. Such a pattern was observed at Sites 501 and 504 near the Costa Rica Rift (Mottl et al., 1983, 1987; Langseth et al., 1987). The pattern at Site 756 does not quite match the pattern seen in the Costa Rica Rift area, however. Theoretically, a concave-upward profile should be seen at the base of Hole 756C and calcium ion concentrations should be nearer seawater values in the upper parts of the sediment column at Hole 756C. If a convection system exists at Site 756, it is more complex than the patterns seen in the Costa Rica Rift region.

A difference is also seen in the calcium profiles in the two Site 757 holes, which are 200 m apart. The relative differences from hole to hole at Site 757 are not as marked as at Site 756. It is more difficult to evaluate the possible causes of the differences at Site 757. With a thicker sediment cover, the likelihood of convection through the sediments is reduced and the scale of the convection system, if it exists, would have to be much larger. The more likely explanation is that basement structure (e.g., fracture spacings below the sediments) changes or the thickness of ash changes. Both of these probably occur (see "Inorganic Geochemistry" section, "Site 757" chapter). Either of these changes could lead to a larger net amount of alteration per unit of time, leading to a higher calcium gradient. Oxygen isotope analyses, to be done on shore, will give a better quantitative estimate of the amount of alteration in the two holes.

At Site 758 no difference was observed in the calcium ion profiles between Holes 758A and 758B. The spacing between the two holes, however, is less than 30 m. Any horizontal differences in the calcium profiles would only exist on a larger scale. In addition, the much greater thickness of sediments at Site 758 makes convection through the sediments highly unlikely and makes any signal diffusing from the lowermost ash sediments, or the basement below, more uniform laterally. If vertical and horizontal diffusivities are comparable, chemical differences created at depth have a greater likelihood of being homogenized laterally in a thicker sediment column.

Overall, the pattern of calcium gradients seen in the pore waters of Sites 756, 757, and 758 fits the changes in age, sediment cover, heat flow, topography, and lithology along Ninetyeast Ridge. At the southernmost site, where sediment cover is thin, the topography is rough, and the heat flow is higher because of the younger age of the basement, chemical changes seem to be highly variable on a small scale. As the age and sediment cover increase to the north, the chemical variability in the pore waters from hole to hole decreases. Of course, local deviations from this pattern are to be expected because topography and basement structure change radically in an east-west direction across the ridge. In general, lateral chemical variations in the pore waters are more pronounced southward.

Much remains to be learned about alteration and fluid flow as it relates to basement structure and sediment cover. Chemical and isotopic studies of pore waters may provide the only method of evaluating these variables on a more detailed scale. To this end, the horizontal spacing of sites or holes should be comparable in distance to the depth of the sediment cover.

CONCLUSIONS

Principal Observations

The principal observations at each site that seem especially important to understanding the Ninetyeast Ridge are listed in the following:

Site 756

1. The age of basement is greater than 38 Ma, based on the age of the overlying sediment.
2. Basement topography is extremely rough near the site.
3. The lavas were erupted subaerially, but this is the only site on Ninetyeast Ridge where basement was reached without penetrating a significant section of volcanic ash and tuff.
4. Large differences were observed in the vertical gradient of the calcium ion concentration between holes only 100 m apart, suggesting that alteration of the basement rocks is very active, perhaps reflecting fluid advection.

Site 757

1. The age of the basement is greater than 58 Ma, based on the age of the overlying sediment.
2. The lavas were probably erupted subaerially.
3. The thick section of pyroclastics came from an eruptive source less than 10 km away. Numerous clinoform shapes on the seismic records indicate either primary bedding planes or the reworking of phreatic deposits at sea level.
4. The geochemistry of the ashes is distinct from that of the basalts.
5. Very strong calcium ion concentrations at the base of the pyroclastic section indicate continuing geochemical alteration.

Site 758

1. The age of the basement is greater than 80 Ma, based on the age of the overlying sediments.
2. Recent faulting is evident in seismic data, but the distribution of geophysical survey tracks is inadequate to resolve a consistent pattern.
3. The lavas were erupted in deep water. Pillows, ponded flows, and sheet flows were drilled.
4. The volcaniclastics in the Upper Cretaceous section include both distal ash falls and turbidity deposits.
5. The geochemistry of the basaltic ashes is distinct from that of the basalts.
6. A regional unconformity corresponds to a major sedimentary hiatus in which almost no Eocene section is present.
7. An excellent tephrochronology of Indonesian arc volcanism is recorded in the late Miocene age and younger section.
8. The upper 100 m of section includes a terrigenous clay component, probably of Himalayan origin, in which is preserved an excellent magnetic reversal stratigraphy for the past 7 m.y. (Brunhes to Chron 6).
9. There was an increase in sedimentation rate in the late Miocene, but this cannot be necessarily attributed to increased runoff from the Himalayas.

Principal Conclusions

The principal conclusions that can be drawn from the present results of drilling on Ninetyeast Ridge are as follows:

1. The volcanism that built Ninetyeast Ridge was probably segregated into volcanic centers forming the higher parts of the ridge topography. Some volcanic activity continued between these centers, as documented at Site 758.
2. The basaltic rocks are not primary magmas derived from the mantle, but are moderately evolved tholeiites. Although there are important intrasite and intersite variations in magma composition, ratios of incompatible elements show that the Ninetyeast Ridge basalts are similar to those found on oceanic plateaus, such as Kerguelen-Heard. Furthermore, trace element abundance ratios fall between those of mid-oceanic ridge and Kerguelen Island basalts, perhaps indicating mantle-source mixing before eruption.
3. All the Ninetyeast Ridge sites received low sediment flux during the Eocene through middle Miocene. These low fluxes occurred at paleopositions between 10° and 40°S when the sites were lying beneath the subtropical gyre of the Southern Hemisphere.

Tectonic Implications

All of the evidence from DSDP and ODP drilling and from regional tectonic models indicates that Ninetyeast Ridge was built by hot-spot volcanism associated with the Kerguelen-Heard Plume, as were the volcanic basements of Broken Ridge and the Kerguelen-Heard Plateau. However, the difficulty comes in developing a tectonic model that accommodates all of the constraints and puts most of the Late Cretaceous and younger volcanic products of the Kerguelen-Heard Plume onto the Indian plate in the form of Ninetyeast Ridge.

Figure 17 shows the position of the center of the Kerguelen-Heard Plume in relation to the ages of the oceanic crust as interpreted by Royer and Sandwell (in press) using all available constraints. The hot spot and the Indian-Antarctic spreading center were reasonably coincident until 69 Ma (Chron 31), when there was a marked increase in spreading rate. As the spreading-center system migrated northward away from Antarctica, which has moved very little relative to the hot spots since the Late Cretaceous, three scenarios were possible:

1. The spreading center was north of the hot spot, but excess volcanism continued at the spreading center in a manner analogous to the Rodriguez-Réunion system. At some subsequent time, the spreading-center segment jumped south to the Kerguelen-Heard Plume source again, and the volcanic trace built on the Antarctic plate was transferred to the Indian plate.
2. The spreading center jumped in many small steps to stay close to the Kerguelen-Heard Plume, transferring the volcanic trace in small parts.
3. The spreading center maintained itself south of the hot spot, allowing the volcanic trace to be built on the Indian plate.

The first scenario is plausible if one can accept the Rodriguez analogy for volcanism at a satellite location fed by subcrustal flow of magma from the main plume. If this occurred, the most likely time for the southward jump of the spreading center is 60 Ma (Chron 26), with the resulting geometry as shown in Figure 18. The implication of this scenario is that the ages of the captured volcanic trace and of the oceanic crust on which it was built should increase to the south. This is a testable hypothesis if the seafloor-spreading anomalies on the fossil microplate are sufficiently coherent to be interpreted.

The second scenario is plausible because it may be thermally favorable for the spreading center to jump frequently (or spread highly asymmetrically) toward the plume source of heat. The implication of this scenario is that the ages of the volcanic trace and of the oceanic crust on which it was built should increase to the north on a macroscopic scale, but on a fine scale they may increase in the opposite direction. It seems unlikely that coher-

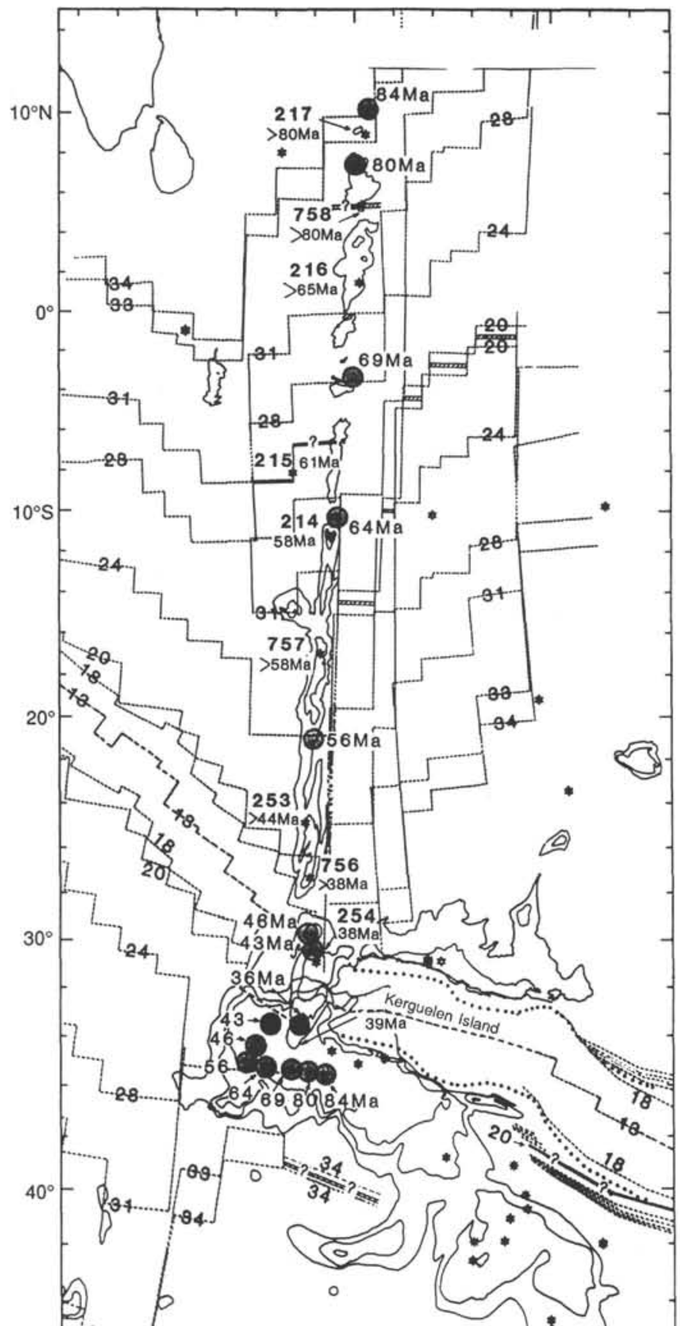

Figure 17. Reconstruction at Chron 13 (36 Ma) showing the location of the Kerguelen/Ninetyeast hot spot (open circles) at Chrons 34 (84 Ma), 33 (80 Ma), 31 (69 Ma), 28 (64 Ma), 24 (56 Ma), 20 (46 Ma), 18 (43 Ma), and 13 (36 Ma; black circle). The Indian and Australian plates are fixed relative to their present-day coordinates. DSDP and ODP sites are indicated by stars, with their corresponding ages. Between 84 and 56 Ma, a westward migration of the Kerguelen/Ninetyeast hot spot relative to Australia is required to maintain the linearity of Ninetyeast Ridge. The predicted ages do not contradict the observed ages; however, between 7° and 14°S, the age progression does not match the interpreted ages of the ocean floor west of Ninetyeast Ridge. From Royer and Sandwell (in press).

ent magnetic anomalies would be preserved from a time of frequent ridge jumps, but such incoherent anomalies could be taken as circumstantial evidence in favor of this scenario.

The third scenario is attractive in that it provides a convenient solution for the uneven distribution of the hot-spot volcanics between the two plates. However, thermal and kinematic considerations indicate that it is unlikely for the spreading center to migrate to a position to the south of the hot spot. Thus, this scenario is considered implausible.

Further Work

Three topics clearly need further work in order resolve the open questions about the origin of Ninetyeast Ridge:

1. More magnetic surveys to resolve the questions of plate kinematics, particularly as related to possible southerly jumps of the Indian-Antarctic spreading-center segment.
2. Side-scan sonar surveys, particularly on the northern half of Ninetyeast Ridge, in order to understand how intraplate deformation has modified the topography of the ridge.
3. Selected drilling holes with basement penetration of 400–500 m in order to penetrate a significant portion of the volcanic pile.

REFERENCES

Bargar, K. F., and Jackson, E. D., 1974. Calculated volumes of individual shield volcanoes along the Hawaiian-Emperor chain. *J. Res. U.S. Geol. Surv.*, 2:545–550.

Bougault, H., Treuil, M., and Joron, J. L., 1979. Trace elements in basalts from 23°N and 36°N in the Atlantic Ocean: fractional crystallization, partial melting, and heterogeneity of the upper mantle. *In* Melson, W. G., Rabinowitz, P. D., et al., *Init. Repts. DSDP*, 45: Washington (U.S. Govt. Printing Office), 493–506.

Chen, C.-Y., and Frey, F. A., 1985. Trace element and isotopic geochemistry of lavas from Haleakala Volcano, east Maui, Hawaii: implications for the origin of Hawaiian basalts. *J. Geophys. Res.*, 90: 8743–8768.

Cheng, Q., Park, K.-H., Macdougall, J. D., Zindler, A., Lugmair, G. W., Hawkins, J., Lonsdale, P., and Staudigel, H., 1987. Isotopic evidence for a hot-spot origin of the Louisville seamount chain. *In* Keating, B. H., Fryer, P., Batiza, R., and Boehlert, G. W. (Eds.), *Seamounts, Islands and Atolls*: Am. Geophys. Union Monogr., 43: 283–296.

Cockerham, R. S., Luyendyk, B. P., and Jarrard, R. D., 1975. Paleomagnetic study of sediments from Site 253 DSDP, Ninetyeast Ridge. *EOS, Trans. Am. Geophys. Union*, 56:978.

Curray, J. R., Emmel, F. J., Moore, D. G., and Raitt, R. W., 1982. Structure, tectonics and geological history of the northeastern Indian Ocean. *In* Nairn, A.E.M., and Stehli, F. G. (Eds.), *The Indian Ocean*: New York (Plenum), 399–450.

Davies, H., Sun, S. S., Frey, F. A., Gautier, I., McCulloch, M., Price, R., Bassias, Y., Klootwijk, C. T., and Leclaire, L., in press. Basalt basement from the Kerguelen Plateau and the trace of a Dupal plume. *Contrib. Mineral. Petrol.*

Detrick, R. S., Sclater, J. G., and Thiede, J., 1977. The subsidence of aseismic ridges. *Earth Planet. Sci. Lett.*, 34:185–196.

Duncan, R. A., 1978. Geochronology of basalts from the Ninetyeast Ridge and continental dispersion in the eastern Indian Ocean. *J. Volcanol. Geotherm. Res.*, 4:283–305.

Dupre, B., and Allègre, C. J., 1983. Pb-Sr isotope variations in Indian Ocean basalts and mixing phenomena. *Nature*, 303:142–146.

Feigenson, M. D., 1986. Constraints on the origin of Hawaiian lavas. *J. Geophys. Res.*, 91:9383–9393.

Fleet, A. J., and McKelvey, B. C., 1978. Eocene explosive submarine volcanism, Ninetyeast Ridge, Indian Ocean. *Mar. Geol.*, 26:73–97.

Frey, F. A., Dickey, J. S., Thompson, G., and Bryan, W., 1977. Eastern Indian Ocean DSDP sites: correlations between petrology, geochemistry and tectonic setting. *In* Heirtzler, J. R., Bolli, H. M., Davies, T. A., Saunders, J. B., and Sclater, J. G. (Eds.), *Indian Ocean Geology and Biostratigraphy*: Washington (Am. Geophys. Union), 189–257.

Frey, F. A., and Roden, M. F., 1987. The mantle source for the Hawaiian Islands: constraints from the lavas and ultramafic inclusions. *In*

Menzies, M., and Hawkesworth, C. (Eds.), *Mantle Metasomatism*: London (Academic Press), 423-463.

Frey, F. A., Wise, W., Garcia, M. O., West, H., Kennedy, A., and Kwon, S. T., in press. Evolution of Mauna Kea Volcano, Hawaii: petrologic and geochemical constraints on postshield volcanics. *J. Geophys. Res.*

Hamelin, B., and Allègre, C. J., 1985. Large-scale units in the depleted upper mantle revealed by an isotopic study of the South-West Indian Ridge. *Nature*, 315:196-199.

Hamelin, B., Dupre, B., and Allègre, C. J., 1986. Pb-Sr-Nd isotopic data of Indian Ocean ridges: new evidence of large scale mapping of mantle heterogeneities. *Earth Planet. Sci. Lett.*, 76:288-298.

Hart, S., 1984. A large-scale isotope anomaly in the Southern Hemisphere mantle. *Nature*, 309:753-757.

Kennett, J. P., 1981. Marine tephrochronology. *In* Emiliani, C. (Ed.), *The Sea: The Oceanic Lithosphere* (vol. 7): Chicago (Wiley), 1373-1436.

Langmuir, C. H., and Hanson, G. N., 1980. An evaluation of major element heterogeneity in the mantle sources of basalts. *Philos. Trans. R. Soc. London A*, 297:383-407.

Langseth, M. L., Mottl, M., Hobart, M. A., and Fisher, A., 1987. The distribution of geothermal and geochemical gradients near Site 501/504: implications for hydrothermal circulation in the oceanic crust. *In* Becker, K., Sakai, H., et al., *Proc. ODP, Init. Repts.*, 111: College Station, TX (Ocean Drilling Program), 23-32.

Lawrence, J. R., and Gieskes, J. M., 1981. Constraints on water transport and alteration in the oceanic crust from the isotopic composition of pore water. *J. Geophys. Res.*, 86:7924-7934.

LeRoex, A. P., Dick, H.J.B., Erlank, A. J., Reid, A. M., Frey, F. A., and Hart, S. R., 1983. Geochemistry, mineralogy and petrologenesis of lavas erupted along the Southwest Indian Ridge, between the Bouvet Triple Junction and 11°E. *J. Petrol.*, 24:267-318.

LeRoex, A. P., Dick, H.J.B., Gulen, L., Reid, A. M., and Erlank, A. J., 1987. Local and regional heterogeneity in MORB from the Mid-Atlantic Ridge between 54.5° and 51°S: evidence for geochemical enrichment. *Geochim. Cosmochim. Acta*, 51:541-555.

Luyendyk, B. P., 1977. Deep sea drilling on the Ninetyeast Ridge: synthesis and a tectonic model. *In* Heirtzler, J. R., Bolli, H. M., Davies, T. A., Saunders, J. B., and Sclater, J. G. (Eds.), *Indian Ocean Geology and Biostratigraphy*: Washington (Am. Geophys. Union), 165-187.

Mahoney, J. J., 1987. An isotopic survey of Pacific Ocean plateaus: implications for their nature and origin. *In* Keating, B. H., Fryer, P., Batiza, R., and Boehlert, G. W. (Eds.), *Seamounts, Islands and Atolls*: Am. Geophys. Union Monogr., 43:207-220.

Mahoney, J. J., Macdougall, J. D., Lugmair, G. W., and Gopalan, K., 1983. Kerguelen hot-spot source for Rajmahal traps and Ninetyeast Ridge? *Nature*, 303:385-389.

Morgan, W. J., 1981. Hotspot tracks and the opening of the Atlantic and Indian oceans. *In* Emiliani, C. (Ed.), *The Sea: The Oceanic Lithosphere* (vol. 7): New York (Wiley), 443-487.

Mottl, M. J., Langseth, M. L., and the Scientific Party of Ocean Drilling Program Leg 111, 1987. Slow hydrothermal circulation through thick sediments confirmed by drilling on south flank of the Costa Rica Rift. *EOS, Trans. Am. Geophys. Union*, 68:1326.

Mottl, M. J., Lawrence, J. R., and Keigwin, L. D., 1983. Elemental and stable-isotope composition of pore waters and carbonate sediments from Deep Sea Drilling Project Sites 501/504 and 505. *In* Cann, J. R., Langseth, M. L., et al., *Init. Repts. DSDP*, 69: Washington (U.S. Govt. Printing Office), 461-486.

Mutter, J. C., and Cande, S. C., 1983. The early opening between Broken Ridge and Kerguelen Plateau. *Earth Planet. Sci. Lett.*, 65:369-376.

Ninkovich, D., 1979. Distribution, age and chemical composition of tephra layers in deep sea sediments off western Indonesia. *J. Volcanol. Geotherm. Res.*, 5:67-86.

Patriat, P., and Achache, J., 1984. India-Eurasia collision chronology has implications for crustal shortening and driving mechanism of plates. *Nature*, 311:615-621.

Peirce, J. W., 1978. The northward motion of India since the Late Cretaceous. *Geophys. J. R. Astron. Soc.*, 52:277-312.

Price, R. C., Kennedy, A. K., Riggs-Sneeringer, M., and Frey, F. A., 1986. Geochemistry of basalts from the Indian Ocean triple junction: implications for the generation and evolution of Indian Ocean Ridge basalts. *Earth Planet. Sci. Lett.*, 78:379-396.

Royer, J.-Y., and Sandwell, D. T., in press. Evolution of the eastern Indian Ocean since the Late Cretaceous: constraints from Geosat altimetry. *J. Geophys. Res.*

Royer, J.-Y., Sclater, J. G., and Sandwell, D. T., in press. A preliminary tectonic chart of the Indian Ocean. *Proc. Indian Acad. Sci., Earth Planet. Sci.*

Ruddiman, W. F., and Glover, L. K., 1982. Mixing of volcanic ash zones in subpolar North Atlantic sediments. *In* Scrutton, R. A., and Talwani, M. (Eds.), *The Ocean Floor*: Chicago (Wiley), 37-67.

Saunders, A. D., 1983. Geochemistry of basalts recovered from the Gulf of California during Leg 65 of the Deep Sea Drilling Project. *In* Lewis, B.T.R., Robinson, P., et al., *Init. Repts. DSDP*, 65: Washington (U.S. Govt. Printing Office), 591-622.

Schlich, R., Wise, S. W., and Shipboard Scientific Party, 1988. That sinking feeling. *Nature*, 334:385-386.

Schilling, J. G., and Noe-Nygaard, A., 1974. Faroe-Iceland mantle plume: rare earth evidence. *Earth Planet. Sci. Lett.*, 21:1-14.

Sclater, J. G., and Fisher, R. L., 1974. The evolution of the east central Indian Ocean, with emphasis on the tectonic setting of the Ninetyeast Ridge. *Geol. Soc. Am. Bull.*, 85:683-702.

Sclater, J. G., von der Borch, C., Veevers, J. J., Hekinian, R., Thompson, R. W., Pimm, A. C., McGowran, B., Gartner, S., Jr., and Johnson, D. A., 1973. Regional synthesis of the Deep Sea Drilling Results from Leg 22 in the eastern Indian Ocean. *In* von der Borch, C. C., Sclater, J. G., et al., *Init. Repts. DSDP*, 22: Washington (U.S. Govt. Printing Office), 815-831.

Stille, P., Unruh, D. M., and Tatsumoto, M., 1986. Pb, Sr, Nd and Hf isotopic constraints on the origin of Hawaiian basalts and evidence for a unique mantle source. *Geochim. Cosmochim. Acta*, 50:2303-2319.

Subbarao, K. V., Hekinian, R., and Chandresekharam, D., 1977. Large ion lithophile elements and Sr and Pb isotopic variations in volcanic rocks from the Indian Ocean. *In* Heirtzler, J. R., Bolli, H. M., Davies, T. A., Saunders, J. B., and Sclater, J. G. (Eds.), *Indian Ocean Geology and Biostratigraphy*: Washington (Am. Geophys. Union), 259-278.

Sun, S. S., and McDonough, W. F., in press. Chemical and isotopic systematics of oceanic basalts: implications for mantle composition and processes. *In* Saunders, A. D., and Norry, M. J. (Eds.), *Magmatism in Ocean Basins*: Spec. Publ. Geol. Soc. London.

Taras, B., and Hart, S. R., 1987. Geochemical evolution of the isotopic and trace element constraints. *Chem. Geol.*, 64:35-54.

Thompson, G., Bryan, W. B., Frey, F. A., and Sung, C. M., 1974. Petrology and geochemistry of basalts and related rocks from Sites 214, 215, 216, DSDP Leg 22, Indian Ocean. *In* von der Borch, C. C., Sclater, J. G., et al., *Init. Repts. DSDP*, 22: Washington (U.S. Govt. Printing Office), 459-468.

Vogt, P. R., 1974. Volcano height and plate thickness. *Earth Planet. Sci. Lett.*, 23:337-348.

Weis, D., Bassias, Y., Gautier, I., and Mennessier, J.-P., 1987a. Isotopic study of MD48 basalts (S. Indian Ocean): Kerguelen type signature. *EOS, Trans. Am. Geophys. Union*, 68:1541.

———, in press. Kerguelen Plateau (South Indian Ocean): isotopic study of MD 48 dredge basalts: Kerguelen-type signature. *Geology*.

Weis, D., Beaux, J. F., Gautier, I., Giret, A., and Vidal, P., 1987b. Kerguelen Archipelago: geochemical evidence for recycled material. *Nato ASI Workshop, Abst., May 25-29, Antalaya, Turkey*, 122-125.

White, W. M., and Hofmann, A. W., 1982. Sr and Nd isotope geochemistry of oceanic basalts and mantle evolution. *Nature*, 296:821.

Ms 121A-115

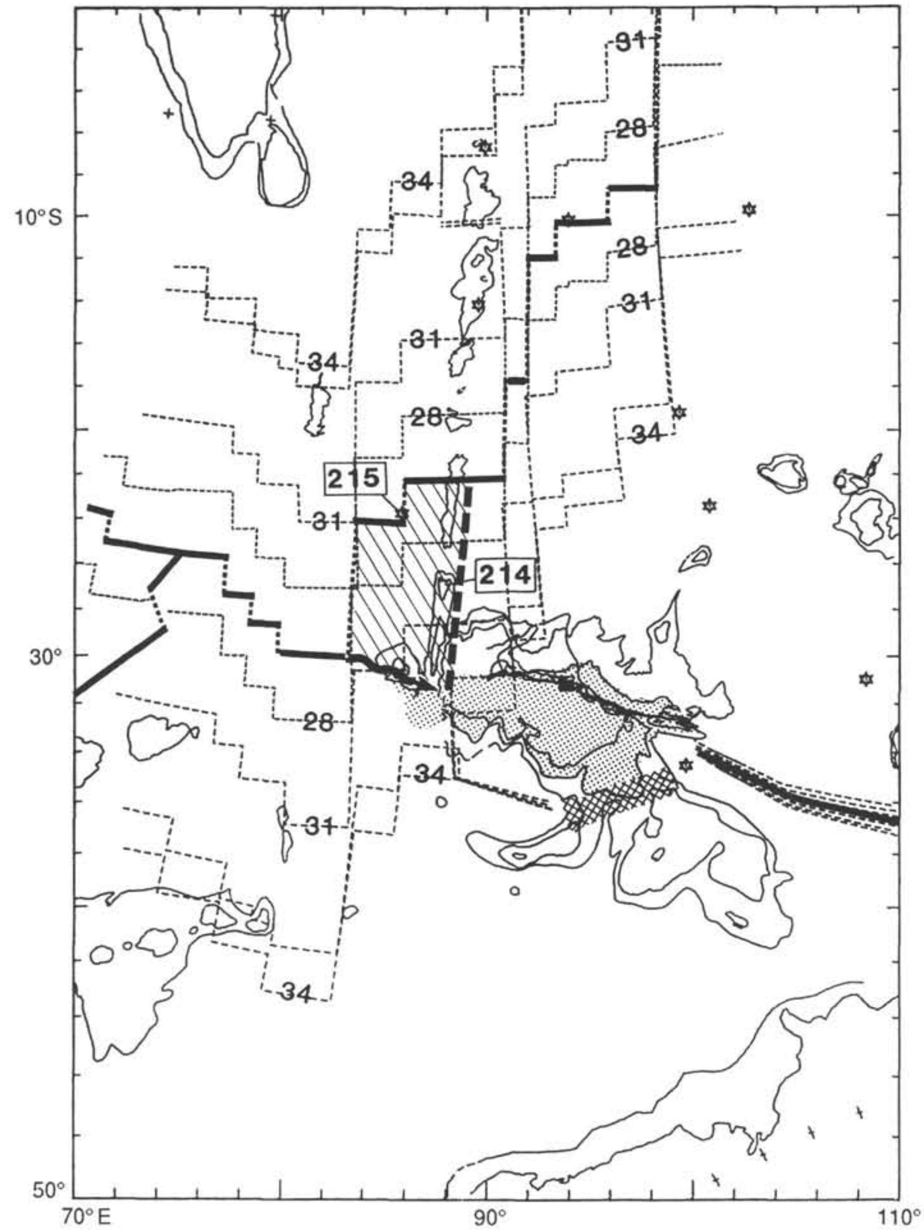

Figure 18. Schematic diagram showing the eastward propagation of the Indian/Antarctic plate boundary through the Kerguelen Fracture Zone at about Chron 26 (60 Ma). Diagonal lines represent the portion of crust that may have been transferred from the Antarctic to the Indian plate. Stippling shows the extent of the combined Broken Ridge/northern Kerguelen Plateau (or Un-Broken Ridge) at 60 Ma. Cross-hatching marks the possible location of the plate boundary between the northern and southern portions of the Kerguelen Plateau. Dashed lines represent isochrons; numbers refer to magnetic anomalies (34 = 84 Ma; 31 = 69 Ma; 28 = 64 Ma). Heavy black lines mark active spreading centers at 60 Ma. Heavy dotted lines delineate active transform faults. From Royer and Sandwell (in press).